

Forward-masked spatial tuning curves in cochlear implant users

David A. Nelson^{a)}

Clinical Psychoacoustics Laboratory, Department of Otolaryngology, University of Minnesota, MMC396, 420 Delaware Street S.E., Minneapolis, Minnesota 55455

Gail S. Donaldson

Department of Communication Sciences and Disorders, University of South Florida, PCD 1017, 4202 E. Fowler Avenue, Tampa, Florida 33620

Heather Kreft

Clinical Psychoacoustics Laboratory, Department of Otolaryngology, University of Minnesota, MMC396, 420 Delaware Street S.E., Minneapolis, Minnesota 55455

(Received 19 March 2007; revised 1 January 2008; accepted 2 January 2008)

Forward-masked psychophysical spatial tuning curves (fmSTCs) were measured in twelve cochlear-implant subjects, six using bipolar stimulation (Nucleus devices) and six using monopolar stimulation (Clarion devices). fmSTCs were measured at several probe levels on a middle electrode using a fixed-level probe stimulus and variable-level maskers. The average fmSTC slopes obtained in subjects using bipolar stimulation (3.7 dB/mm) were approximately three times steeper than average slopes obtained in subjects using monopolar stimulation (1.2 dB/mm). Average spatial bandwidths were about half as wide for subjects with bipolar stimulation (2.6 mm) than for subjects with monopolar stimulation (4.6 mm). None of the tuning curve characteristics changed significantly with probe level. fmSTCs replotted in terms of acoustic frequency, using Greenwood's [J. Acoust. Soc. Am. **33**, 1344–1356 (1961)] frequency-to-place equation, were compared with forward-masked psychophysical tuning curves obtained previously from normal-hearing and hearing-impaired acoustic listeners. The average tuning characteristics of fmSTCs in electric hearing were similar to the broad tuning observed in normal-hearing and hearing-impaired acoustic listeners at high stimulus levels. This suggests that spatial tuning is not the primary factor limiting speech perception in many cochlear implant users.

© 2008 Acoustical Society of America. [DOI: 10.1121/1.2836786]

PACS number(s): 43.64.Me, 43.66.Fe, 43.66.Dc, 43.66.Mk [AJO]

Pages: 1522–1543

I. INTRODUCTION

A multichannel cochlear implant is designed to take advantage of the tonotopic arrangement of auditory nerve fibers within the cochlea. Under ideal circumstances, the current delivered through a given electrode stimulates a discrete group of auditory nerve fibers that reside close to that electrode. This allows information in adjacent frequency bands of the acoustic stimulus to be transmitted to adjacent groups of auditory nerve fibers, roughly mimicking tonotopic stimulation patterns in acoustic hearing. In practice, however, at least two factors can alter the desired “electrotopic” (electrode-to-place) mapping. First, cochlear implant users may have irregular patterns of auditory nerve survival (Hinojosa and Lindsay, 1980; Spoendlin and Schrott, 1988; Zappia *et al.*, 1991; Nadol *et al.*, 2001). If no nerve fibers exist near a particular electrode, then current delivered through that electrode will necessarily stimulate auditory fibers that are apical and/or basal to the intended location. Second, structural changes to the cochlea following deafness and cochlear implantation may result in irregularities in the impedance pathways that govern current flow (Spelman *et al.*, 1982; Black *et al.*, 1983; Shepherd *et al.*, 1994; Jolly, 1998;

Hughes *et al.*, 2001; Saunders *et al.*, 2002). This may result in stimulation of auditory nerve fibers remote from the electrode contact in either the apical or basal direction. In either case, neural excitation may be displaced from the intended neural targets.

Sound perception through a cochlear implant may also be affected by the spatial extent of current fields delivered through individual electrode contacts. The “spatial selectivity” of these current fields determines the degree of overlap between adjacent frequency channels, thereby influencing the maximum spectral resolution that can be supported by the device. The spatial selectivity of current fields is primarily determined by the mode of electrical coupling, with bipolar coupling producing narrower current fields than monopolar coupling. However, the corresponding neural activation patterns are influenced by additional factors, such as the density of neurons in particular regions of the cochlea, and the radial distance between the electrode array and neural targets in the modiolus (Kral *et al.*, 1998; Liang *et al.*, 1999; Cohen *et al.*, 2001; Saunders *et al.*, 2002; Skinner *et al.*, 2002; Cohen *et al.*, 2003). Since these parameters vary across individuals, they can be expected to result in varying degrees of neural spatial selectivity across individual cochlear implant users, even when the mode of electrode coupling is held constant.

^{a)}Electronic mail: dan@umn.edu

Together the two factors just described—aberrations in the electrotopic map and limited spatial selectivity—reduce spectral resolution by restricting the amount and accuracy of spectral information that can be transmitted to cochlear implant listeners. Given the critical role that spectral cues play in sound perception, these factors also represent key limitations to overall device benefit. It may be possible to partly compensate for reduced spectral resolution by using alternative modes of stimulation, such as tripolar stimulation (Jolly *et al.*, 1996; Kral *et al.*, 1998; Morris and Pfingst, 2000; Bierer, 2007) and dual-electrode stimulation (McDermott and McKay, 1994; Wilson *et al.*, 1994; Busby and Plant, 2005; Donaldson *et al.*, 2005; Dingemans *et al.*, 2006), or by devising custom frequency-to-electrode mappings for individual users. However, robust measures of spatial selectivity are needed to evaluate the effectiveness of such approaches.

In acoustic hearing, the forward-masked psychophysical tuning curve (fmPTC) has been used to evaluate the frequency selectivity of the auditory system and to identify irregularities in the tonotopic map. Frequency selectivity has been quantified by measuring the slopes of the apical and basal sides of the fmPTC and by computing the relative bandwidth (Q value) of the fmPTC at some criterion level above its tip (e.g., Nelson and Freyman, 1984; Nelson, 1991). Irregularities in the tonotopic map have been documented by evaluating fmPTC tip frequencies. Tips that are displaced in frequency signify “dead regions” in the cochlea where hair cells are no longer functional and amplification may not be effective (Moore *et al.*, 2000; Moore, 2001; Moore and Alcantara, 2001).

In electric hearing, forward masking has been used to evaluate spatial selectivity in the form of spatial masking patterns. However, these masking patterns involve relatively high masker amplitudes (Lim *et al.*, 1989; Fu *et al.*, 1997; Chatterjee and Shannon, 1998; Collins and Throckmorton, 1998; Cohen *et al.*, 2001; Boex *et al.*, 2003; Dingemans *et al.*, 2006; Kwon and van den Honert, 2006), which preclude the assessment of tuning in localized regions of the cochlea. Therefore, in this paper, we introduce a new measure that is a variation of the acoustic fmPTC. This measure, which we call the *forward-masked spatial tuning curve* (fmSTC), utilizes low-level probes to quantify spatial selectivity and assess electrotopic aberrations in localized regions of the surviving neural array within the cochlea. The measurement paradigm is similar to that used to measure fmPTCs, allowing us to directly compare spatial tuning in electric hearing with frequency tuning in acoustic hearing. In acoustic hearing, tuning curves are extremely narrow at low stimulus levels, owing to nonlinear processes associated with cochlear outer hair cells (e.g., Nelson *et al.*, 2001; Nelson and Schroder, 2004). At higher stimulus levels, the cochlea is dominated by passive mechanical processes, and tuning curves are substantially broader (Nelson, 1991). Since electrical stimulation bypasses the cochlea, such nonlinear behaviors should not be observed in electrically stimulated fmSTCs. Instead, electrical stimulation should produce tuning curves that are essentially constant with level. The slopes and bandwidths of these tuning curves should reflect the attenuation character-

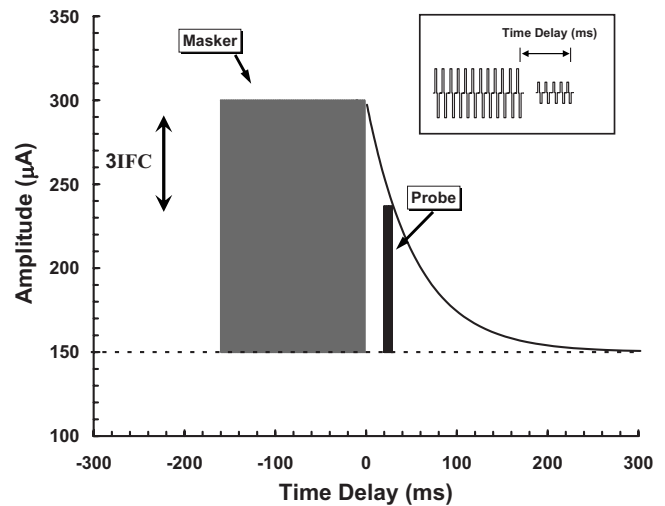


FIG. 1. Schematic diagram of the forward-masking paradigm used to obtain spatial tuning curves. Masker/probe amplitude (μA) is shown as a function of time (ms) relative to the offset of the masker pulse train. Masker and probe biphasic pulse trains are depicted by the inset. Probe threshold is shown by the horizontal dashed line. The masker pulse train is shown by the shaded rectangle, and the probe pulse train is shown by the black narrow rectangle. Expected recovery from forward masking, as a function of time delay, is depicted by the exponential curve following the masker. The probe pulse train is fixed in level at a predetermined time delay and the amplitude of the masker pulse train is adjusted (with a 3IFC adaptive procedure) until the masker just masks the probe.

istics of the current stimulus and patterns of surviving neurons, rather than mechanical properties of the cochlea.

The goals of the present study are: (1) to characterize fmSTCs for probe electrodes near the middle of the electrode array in cochlear implant users stimulated with either a bipolar electrode configuration (Nucleus N22 subjects) or a monopolar electrode configuration (Clarion C-I or C-II subjects); (2) to confirm that probe level has no systematic effect on fmSTC slopes; and (3) to compare fmSTC-based measures of spatial selectivity in cochlear implant listeners to previously reported fmPTC-based measures of frequency selectivity in normal-hearing and hearing-impaired acoustic listeners.

II. METHODS

A. Stimuli and procedures

1. Forward-masking paradigm

Our procedure for obtaining fmSTCs uses a forward-masking paradigm (Shannon, 1983a, 1986, 1990a; Chatterjee and Shannon, 1998; Chatterjee, 1999; Nelson and Donaldson, 2002) to measure a constant amount of forward masking on a specific *probe* electrode, for multiple *masker* electrodes surrounding that probe. This paradigm is illustrated in Fig. 1. A short train of probe pulses is presented at a fixed time delay following a longer train of masker pulses. The masker is presented in three sequential listening intervals, and the probe follows the masker in one randomly chosen interval. The subject’s task is to choose the interval that contains the probe stimulus. The amplitude of the probe stimulus is fixed in level, and the amplitude of the masker stimulus is adjusted (vertical double arrow) using an adaptive procedure (de-

scribed in the following), until the amount of forward masking produced is just sufficient to mask the probe. In Fig. 1, the time course of recovery from forward masking is represented by the black curve. In this study, the masker duration was 160 ms, the time delay was 20 ms, and the probe duration was 10 ms. As indicated in the inset to Fig. 1, time delay was specified as the time between masker offset and probe offset, because the final portion of the probe primarily determines the probe detection threshold in forward masking (Nelson and Donaldson, 2002).

For Nucleus subjects, experiments were carried out using a computer linked to a specialized cochlear implant interface (Shannon *et al.*, 1990). For Clarion subjects, experiments were carried out using a computer with a special-purpose microprocessor that controlled a dedicated speech processor (Clarion Research Interface). The stimuli used for Nucleus subjects were trains of 500-Hz biphasic current pulses. The biphasic pulses were cathodic first (relative to the active electrode), with a per-phase pulse duration of 200 μ s and an interphase delay of 44 μ s. Stimulus amplitudes were specified in clinical amplitude steps, called *current step units* or CSUs, which are uneven amplitude steps that vary between 0.07 and 0.30 dB for the range of current amplitudes used here. CSUs were converted to calibrated current amplitudes (μ A) using subject-specific tables provided by Cochlear Corporation. One Nucleus subject (N09) was tested as part of an earlier study that used different stimulation and forward-masking parameters. For this subject, stimuli were trains of 125-Hz biphasic pulses, masker duration was 256 ms, probe duration was 32 ms, and the time delay between masker and probe was 42 ms.

For the Clarion subjects, stimuli were trains of 500-Hz biphasic current pulses, with a per-phase duration of 77 μ s and no delay between phases. Stimulus amplitudes were specified in clinical amplitude steps, called *stimulus units* or SUs, which are logarithmic amplitude steps of 0.15–0.30 dB. SUs were translated to calibrated amplitudes (μ A) using a set of look-up tables developed in our laboratory. These tables compensate for nonlinearities in the current source that depend upon electrode impedance and pulse rate. Electrode impedances for Clarion subjects were measured at the beginning and end of each data collection session. The impedances measured for individual subjects typically varied less than 10% across sessions. Variance associated with impedance measurements can produce up to 10% error in calibrated amplitudes for Clarion C-I subjects, but has essentially no effect on calibrated amplitudes for Clarion C-II subjects, due to the improved current source incorporated in the C-II device. The variance associated with the impedance measurements will, of course, be reflected in the variability of the forward-masked thresholds, as represented by error bars shown for individual fmSTCs in later figures.

2. Absolute thresholds and maximum acceptable loudness levels

Prior to obtaining fmSTCs for a particular probe electrode, absolute detection threshold (THSp) and maximum acceptable loudness level (MALp) were determined for the

10-ms probe pulse train. THSp was measured with a three-interval forced choice (3IFC) adaptive procedure similar to that used for measuring masked thresholds (described in the following), but only one interval contained the probe stimulus and the other two contained silence. MALp was measured with an ascending method of limits procedure in which pulse trains, presented at a rate of 2/s, were slowly increased in amplitude until the subject indicated that loudness had reached a “maximum acceptable” level. Estimates for two consecutive ascending runs were averaged to obtain a single measure of MALp. THSp and MALp were measured at the start of each test session for the probe electrode to be evaluated in that session, and THSp was measured again at the end of the test session. Corresponding measures of threshold (THSm) and maximum acceptable loudness level (MALm) were obtained for all masker electrodes, using the 160-ms masker pulse train. These measures were obtained both before and after the measurement of a series of fmSTCs at different probe levels. The values of THSm and MALm reported here represent the average of measures obtained across all data collection sessions for a given subject.

3. Adaptive masked-threshold procedure

As mentioned earlier, forward-masked thresholds were obtained using a 3IFC adaptive procedure. The masker pulse train was presented in each of three listening intervals. The probe pulse train was presented in one of the three intervals, chosen randomly from trial to trial, at a fixed time delay following the masker. The subject’s task was to choose the “different” interval by pressing the appropriate button on a three-button computer mouse or by selecting one of three colored squares on a video screen using a standard mouse. Stimulus intervals were cued by the appearance of the three squares on the video screen, and correct-answer feedback was provided after each trial. The amplitude of the masker pulse train was initially set to a level 2–4 dB below the anticipated masked threshold. Masker amplitude was adjusted on subsequent trials using a two-up, one-down stepping rule that estimated the stimulus level corresponding to 70.7% correct discrimination (Levitt, 1971). For the first four reversals in the direction of amplitude changes, masker level was varied in 1-dB steps (0.5-dB steps in a few subjects with very small dynamic ranges). These initial reversals quickly moved the adaptive track into the target region for masked threshold. After the fourth reversal, step size was reduced, typically to one-fourth of the initial step size, and remained constant for all remaining trials. Trials continued until a total of 12 reversals occurred. The mean of the final 8 reversals was taken as the masked threshold.

Masked thresholds were determined in this manner for maskers on electrodes surrounding and including the probe electrode. Testing began with the masker on the probe electrode and proceeded to sequentially more apical or more basal maskers. The order of testing electrodes (apical-direction-first versus basal-direction-first) was alternated on consecutive retests. Retests continued in the initial and subsequent test sessions until three or more masked thresholds

TABLE I. Subject information. Gender, age when tested, etiology of deafness, duration of bilateral severe-to-profound hearing loss prior to implantation, duration of implant use prior to the study, implanted device with electrode type (SPRL=spiral; HF=HiFocus; HFP=HiFocus with positioner) for Clarion users only, and insertion depth.

Subject	M/F	Age	Etiology	Duration (years)	CI Use (years)	Device (electrode type)	Depth (mm)
C03	F	53.4	Progressive, familial	27	4.2	C-I (SPRL)	25
C05	M	47.8	Unknown, sudden	<1	5.6	C-I (SPRL)	25
C16	F	50.1	Progressive	13	2.6	C-I (HF)	25
C18	M	71.4	Otosclerosis	33	4.6	C-I (HFP)	25
C23	F	42.7	Progressive	27	1.1	C-I (HFP)	25
D08	F	54.7	Otosclerosis	13	3.8	C-II (HF)	25
N09	M	67.4	Meniere's disease	1	10.6	N22	22
N13	M	65.2	Progressive, familial	4	12.8	N22	24
N14	M	58.0	Progressive	1	8.4	N22	25
N28	M	65.6	Meningitis	<1	8.6	N22	25
N32	M	37.2	Maternal rubella	<1	7.4	N22	23
N34	F	57.9	Mumps, progressive	9	4.4	N22	22

were obtained for each masker electrode. Each point on the fmSTC was based on the average of three to five forward-masked thresholds.

B. Subjects and electrodes

Subjects were 12 postlingually deafened adults, 6 implanted with a Nucleus 22 device (Patrick and Clark, 1991), 5 implanted with a Clarion C-I device (Schindler and Kessler, 1993; Kessler, 1999), and 1 implanted with a Clarion C-II device (Frijs et al., 2002). The Nucleus users were implanted with a 22-electrode straight array. The Clarion users were implanted with a 16-electrode Spiral array (SPRL), a 16-electrode HiFocus array (HF), or a 16-electrode HiFocus array with an electrode positioning system (HFP). Table I displays relevant information for each subject including gender, age, etiology of deafness, duration of hearing loss prior to implantation, duration of implant use prior to participation in the study, electrode type (Clarion users), and insertion depth.

For each of the 12 subjects, a fmSTC was obtained for a probe electrode near the middle of the array. Two to four probe levels were assessed at current amplitudes between 8% and 33% of the probe dynamic range in microamperes ($DR_{\mu A}$).

Nucleus subjects were stimulated in bipolar mode, using an electrode separation of 0.75 mm (BP), or the narrowest separation greater than 0.75 mm [either 1.5 mm (BP+1) or 2.25 mm (BP+2)] that allowed MALp and MALm to be achieved at current amplitudes that could be produced by the device. Nucleus electrodes were numbered sequentially from 1 to 22, beginning with the most apical electrode. This numbering scheme is in reverse order from the one used clinically.

Clarion subjects were stimulated in monopolar mode. The Clarion Spiral electrode array (SPRL) incorporates 8 pairs of lateral and medial electrodes. For this array, electrodes were numbered sequentially from 1 to 16, beginning with the most apical electrode; thus all odd-numbered electrodes were lateral electrodes and all even-numbered elec-

trodes were medial electrodes. For subjects with the Clarion C-I receiver and SPRL array (C03 and C05), only medial electrodes were stimulated, which were separated by 2.0 mm. The Clarion HiFocus electrode array (HF) incorporates 16 electrodes in a linear arrangement; these electrodes were numbered 1–16, beginning with the most apical electrode. Subjects with the Clarion C-I receiver and HF array (C16, C18, and C23) were stimulated on the same electrodes used in their clinical speech-processor programs (either all even-numbered or all odd-numbered electrodes), which were separated by 2.2 mm. The remaining electrodes were not used because lack of regular stimulation resulted in high electrical impedances. One subject with the Clarion C-II receiver and HF array (D08) was tested on all 16 electrodes, which were separated by 1.1 mm.

Because the electrode-numbering schemes used here differ in some cases from clinical numbering schemes, electrode numbers are specified using the prefix “rEL”, to indicate research electrode numbering.

C. Parameters of the fmSTC

Figure 2 shows an example fmSTC from a Nucleus subject. Figure 2 will be used to familiarize the reader with our standard format for presenting fmSTCs and with the quantitative measures used to describe them.

Probe electrode: The heading on the graph specifies the subject (N14), the probe electrode pair (rEL12:11), and the electrode configuration of the probe (BPp) and the masker (BPm) used to generate the fmSTC. The x axis shows electrode number, with more apical electrodes toward the left and more basal electrodes toward the right. The y axis shows stimulus amplitude in microamperes. The horizontal positions of the open circle and arrow identify the active and reference electrodes, respectively, of the bipolar probe; the vertical level of these symbols indicates the probe level (in microamperes) used to obtain the fmSTC. The level of the horizontal bar connecting the probe and reference electrodes indicates the absolute threshold of the probe (THSp), which was 488 μA in this example. If monopolar stimulation had

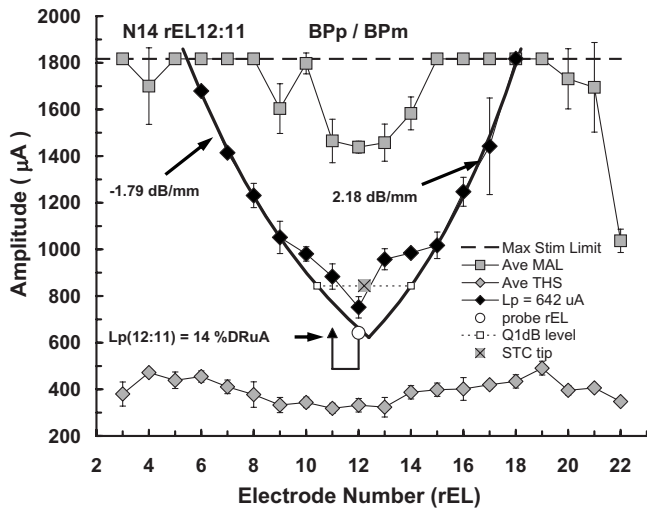


FIG. 2. Example forward-masked spatial tuning curve (fmSTC) from a Nucleus subject. Stimulus amplitude (μA) is shown on the ordinate; research electrode number (rEL) is shown on the abscissa. The rEL numbering system assigns 1 to the most apical electrode with consecutive numbering proceeding to the basal electrode. Average maximum acceptable loudness (Ave MAL) levels obtained with the masker stimulus are shown as shaded squares. Standard deviations are shown by the error bars. The dashed line across the top of the graph indicates the maximum current amplitude that can be generated by this subject's device. Average 3IFC thresholds (Ave THS) obtained with the masker stimulus are shown by the shaded diamonds, because this subject used a Nucleus device, stimuli were delivered in bipolar mode. The horizontal positions of the open circle and closed triangle identify the "active" and "reference" probe electrodes, respectively; probe level is indicated by the vertical position of these two symbols, with the height of the vertical lines indicating the sensation level of the probe; the horizontal line below the symbols indicates the subject's absolute threshold for the probe stimulus. For each fmSTC, masker levels required to forward-mask the probe stimulus, at each masker electrode, are shown by the closed black symbols. Masked thresholds were obtained for all testable electrodes, but those that reached the subject's MAL (or the maximum stimulation limit of the device) on any electrode are not plotted in the graphs. Heavy solid curves on each side of the fmSTC show the logarithmic fitted slopes. Slope values are often specified next to each curve. In this example fmSTC, the results of the bandwidth calculation are shown: The dashed line shows the level 1 dB above the tip, and the open squares show the apical and basal limits of the bandwidth measure. The fmSTC tip calculation is shown in this example by the shaded \times symbol. Labels at the top of the graph indicate the subject code (N14), the probe electrode (rEL12:11) (active:reference research electrode numbers), and the mode of stimulation for the probe and masker (BPP/BPm).

been used, then the probe electrode would be indicated by a single open circle and a vertical bar extending to the level of the probe threshold. Because the probe electrode is fixed in level, and because the stimulus amplitude on the probe is relatively low, it is assumed that the probe is exciting a constant, relatively small population of neurons that may or may not be close to the probe electrode.

The absolute threshold of the probe (represented by the horizontal bar) was typically higher than the absolute threshold for the masker on the same electrode. This can be attributed to temporal integration (Donaldson *et al.*, 1997), since the masker duration was approximately ten times greater than the probe duration.

Masker electrodes: The plot of forward-masked thresholds across electrodes defines a fmSTC. In this example, forward-masked thresholds are represented by the solid diamonds. The corresponding legend entry indicates the level of

the probe used to obtain these thresholds ($L_p=642 \mu\text{A}$). Forward-masked thresholds were always determined for all test electrodes in the array; however, for clarity, forward-masked thresholds that reached the MALm on a particular masker electrode are not plotted. The fmSTC defines a spatial region over which masker stimuli interfere with the perception of the probe stimulus. Masker stimuli within and above the fmSTC function mask the probe; those outside and below the function do not.

Average values of MALm and THSm are shown by the shaded squares across the top of the graph and the shaded diamonds across the bottom of the graph, respectively. Error bars indicate 1 s.d. above and below each value. The dashed line across the top of the graph indicates the maximum current amplitude that can be generated by this subject's device. Maximum stimulation limits are relevant only for subjects with the Nucleus implant, and vary across individuals according to the calibration tables provided by Cochlear Corp.

Slopes, bandwidths, and tip shifts: In order to quantify spatial tuning characteristics across subjects and probe levels, each fmSTC was fitted with two logarithmic functions, one on the apical side and one on the basal side. As indicated by the heavy solid curves in Fig. 2, only the steepest portion of each side was included in the least-squares fit. Typically, the function included three or more masked thresholds. However, in cases of extremely steep slopes, or when the tested electrodes had larger physical separations, only two masked thresholds were sometimes included. The fitted slopes were expressed in units of dB/mm. The spatial bandwidth of the fmSTC was calculated as the distance (in millimeters) between the apical and basal fitted slopes at an amplitude 1 dB above the lowest masker level. We refer to this measure as the fmSTC *bandwidth*. In Fig. 2, bandwidth is represented by the two open squares connected by a dashed line. The fmSTC *tip place*, illustrated by the shaded \times symbol, was specified at the midpoint of the bandwidth, and the *tip shift* was specified as the difference between the tip place and the probe electrode place (in millimeters). These procedures for quantifying fmSTCs focus on the steepest portion of the function and ignore irregularities that sometimes occurred close to the probe electrode. Such irregularities were common among the Nucleus subjects tested in bipolar mode, and will be described later for individual subjects.

Statistical analysis. The effect of probe level on each fmSTC parameter (apical or basal slope, bandwidth, or tip shift) was evaluated by performing a linear regression on that parameter as a function of probe amplitude, with probe amplitude specified as a percentage of probe dynamic range in microampere ($\%DR\mu\text{A}$). Separate regression analyses were performed for monopolar (Clarion) and bipolar (Nucleus) subjects. The effect of subject group (monopolar versus bipolar) was evaluated by first computing the average parameter value across probe levels for each subject, and then performing a two-tailed T-test to assess differences between the two groups. The use of average data (collapsed across probe level) for individual subjects was justified because probe level was found to have no systematic effect on fmSTC parameters for either group.¹

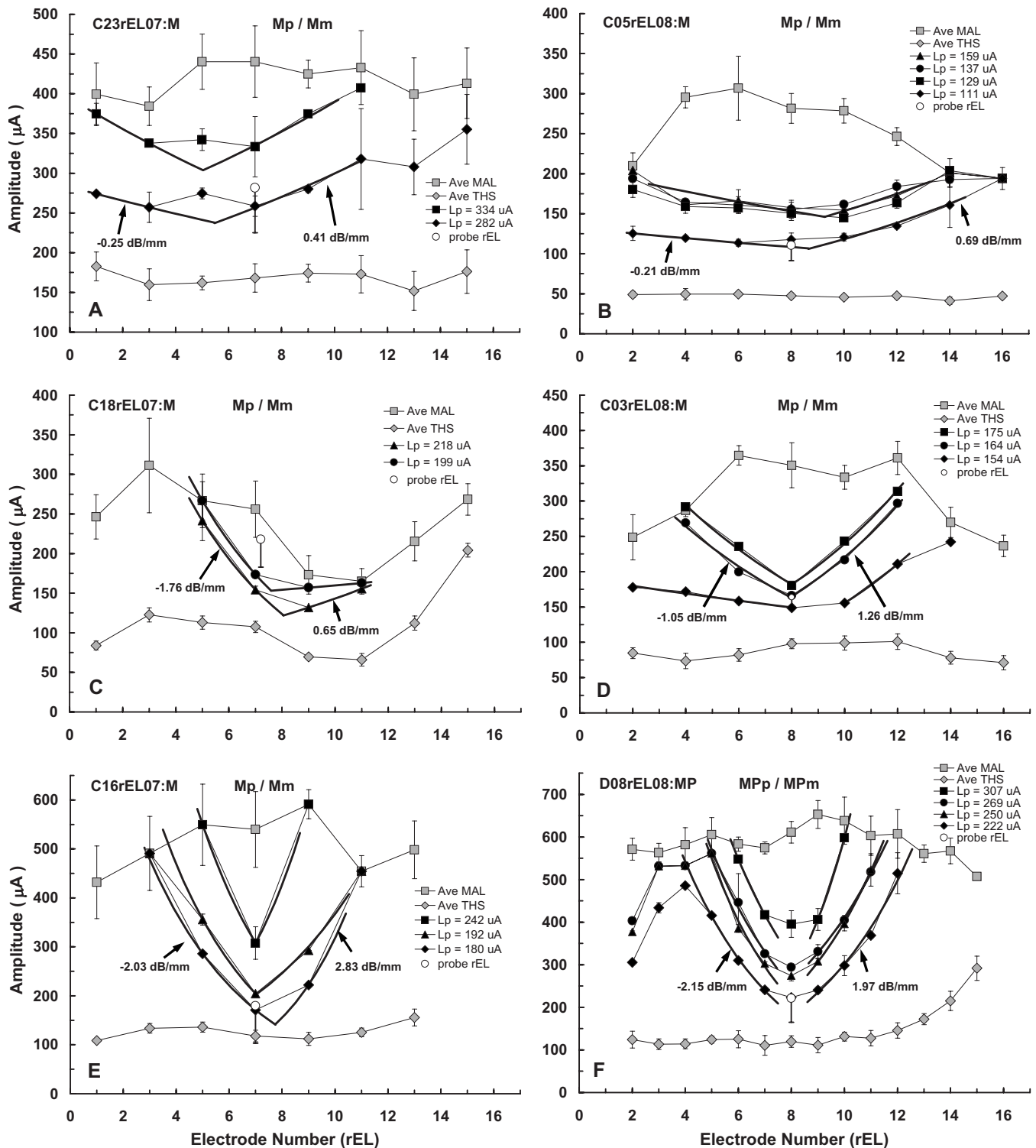


FIG. 3. fmSTCs for six Clarion cochlear-implant users who were stimulated using a monopolar electrode configuration. The horizontal position of the open circle in each graph identifies the probe electrode; probe level is indicated by the vertical position of this symbol, with the height of the vertical line indicating the sensation level of the probe; the horizontal line below the open circle indicates the subject's absolute threshold for the probe stimulus. For clarity, only the lowest probe level is plotted. Other features of the individual graphs are the same as those described for Fig. 2.

III. RESULTS AND DISCUSSION

A. Characteristics of fmSTCs in electrical hearing

Figure 3 shows fmSTCs obtained at two or more probe levels from each of the six Clarion subjects. These fmSTCs were obtained using a monopolar probe and a monopolar masker (MPP/MPm). Thresholds for the masker stimulus

ranged between 50 and 200 µA, and corresponding MALs ranged between 200 and 650 µA. For purposes of clarity, only the lowest probe level is shown on each graph (open circle); however, all probe levels (Lp) are specified in the graph legends. The slopes, bandwidths, and tip-shift parameters for each of the fmSTCs are given in Table II.

TABLE II. Spatial tuning curve parameters in Clarion subjects.

Subject probe rEL	Ave Lp (%DR μ A)	Slopes (dB/mm)		Bandwidth (mm)	Tip shift (mm)	Ap/Am (dB)
		Apical	Basal			
C23rEL07:M	34	-0.41	0.40	9.00	-2.11	0.0
	15	-0.25	0.41	9.09	-1.54	0.7
C05rEL08:M	31	-0.32	0.57	7.18	0.27	0.1
	21	-0.30	0.38	7.48	-0.34	-1.1
	17	-0.21	0.74	6.70	0.19	-1.4
	8	-0.21	0.69	9.64	-1.86	-0.5
C18rEL07:M	20	-1.76	0.65	3.51	1.97	3.0
	8	-1.70	0.14	5.03	2.44	1.2
C03rEL08:M	21	-1.04	1.20	1.67	-0.05	-0.3
	17	-1.05	1.26	1.96	-0.13	-0.1
	14	-0.27	1.31	6.05	-0.57	0.3
C16rEL07:M	24	-2.29	2.58	0.83	-0.02	-2.1
	13	-2.19	1.58	1.16	0.13	-0.6
	11	-2.03	2.83	2.25	0.63	0.4
D08rEL08:MP	29	-2.15	3.05	2.70	0.00	-2.2
	21	-2.15	1.77	2.22	0.02	-0.8
	17	-2.44	2.09	2.37	-0.06	-0.8
Ave (C)	18.9	-1.22	1.27	4.64	-0.06	-0.2
Sdev (C)	7.5	0.89	0.92	3.05	1.15	1.2
Min (C)	7.6	-0.21	0.14	0.83	-2.11	-2.2
Max (C)	33.5	-2.44	3.05	9.64	2.44	3.0

A range of fmSTC shapes was exhibited by the Clarion users. Subjects C23 and C05 [Figs. 3(A) and 3(B)] exhibited very shallow slopes and broad spatial tuning, with slopes ranging between 0.2 and 0.6 dB/mm, and bandwidths ranging between 7.0 and 9.6 mm (not shown in Fig. 3, but given in Table II). At the other extreme, subjects C16 and D08 [Figs. 3(E) and 3(F)] exhibited relatively steep slopes and narrow tuning, with slopes ranging between 1.6 and 3.0 dB/mm, and bandwidths ranging between 0.8 and 2.7 mm. Subjects C18 and C03 [Figs. 3(C) and 3(D)] demonstrated intermediate slopes and bandwidths.

For three of the Clarion subjects in Fig. 3 (C03, C16, D08), the tips of tuning curves (lowest masker levels) were located very close to the probe electrode, suggesting that neurons stimulated by the probe stimulus were proximal to the probe electrode. Note that subject D08 [Fig. 3(F)] demonstrated a downturn in masked thresholds for apical maskers rEL02 and rEL03. This may be attributable to a bending-over of the tip of her electrode array (visualized on x ray) and an associated pitch-reversal on rEL02 and rEL03 (Donaldson *et al.*, 2005). The other three subjects represented in Fig. 3 (C23, C05, and C18) exhibited varying degrees of mistuning, or displacement between the probe electrode and the tuning curve tip. Subjects C23 and C05 [Figs. 3(A) and 3(B)] exhibited minor mistuning with fmSTC tips that were shifted 1.5–2.1 mm in the apical direction and 0.6–1.9 mm in the basal direction, respectively. However, the extremely shallow slopes in these subjects resulted in some uncertainty as to “true” tip locations. Subject C18 [Fig. 3(C)] exhibited moderate mistuning, with the fmSTC tips shifted 2.4–3.6 mm in the basal direction. For this subject,

fmSTC shape may have been influenced by irregular MALM values, which were considerably lower on electrodes rEL09 and rEL11 than on other electrodes.

For most subjects, the fmSTC tip level increased with increasing probe level, i.e., masker amplitude grew with probe amplitude. However, notice that fmSTC amplitudes actually decreased with increasing probe amplitude for subject C18 [Fig. 3(C)]. This is likely explained by fluctuations in probe thresholds over the long testing period required to collect the data for this subject. The probes used to generate these curves had amplitudes corresponding to 15% and 27% (triangles and circles, respectively) of the dynamic range measured on the days that testing was completed; thus, masker amplitudes grew with probe sensation level (expressed as %DR μ A). Subject C03 [Fig. 3(D)] exhibited extremely broad spatial tuning at the lowest probe level tested, despite the fact that the probe level was well above threshold at 15 %DR μ A. Such extremely broad tuning was also observed during pilot testing with several other subjects, but only when very low probe levels were used (e.g., see subject N32 in Fig. 4).

Figure 4 shows the fmSTCs obtained at two or more probe levels in each of the six Nucleus subjects. For three of these subjects (N14, N34, N32), fmSTCs were obtained using a bipolar probe and a bipolar masker (BPp and BPm; both with 0.75-mm spatial separation between active and reference electrodes). For two other subjects (N28 and N13), the BP maskers did not produce sufficient forward masking to mask the probe stimulus. Therefore, the electrode separation of the BP masker was increased to BP+1 or BP+2 (1.5 or 2.25 mm).² The remaining subject (N09) was tested with a

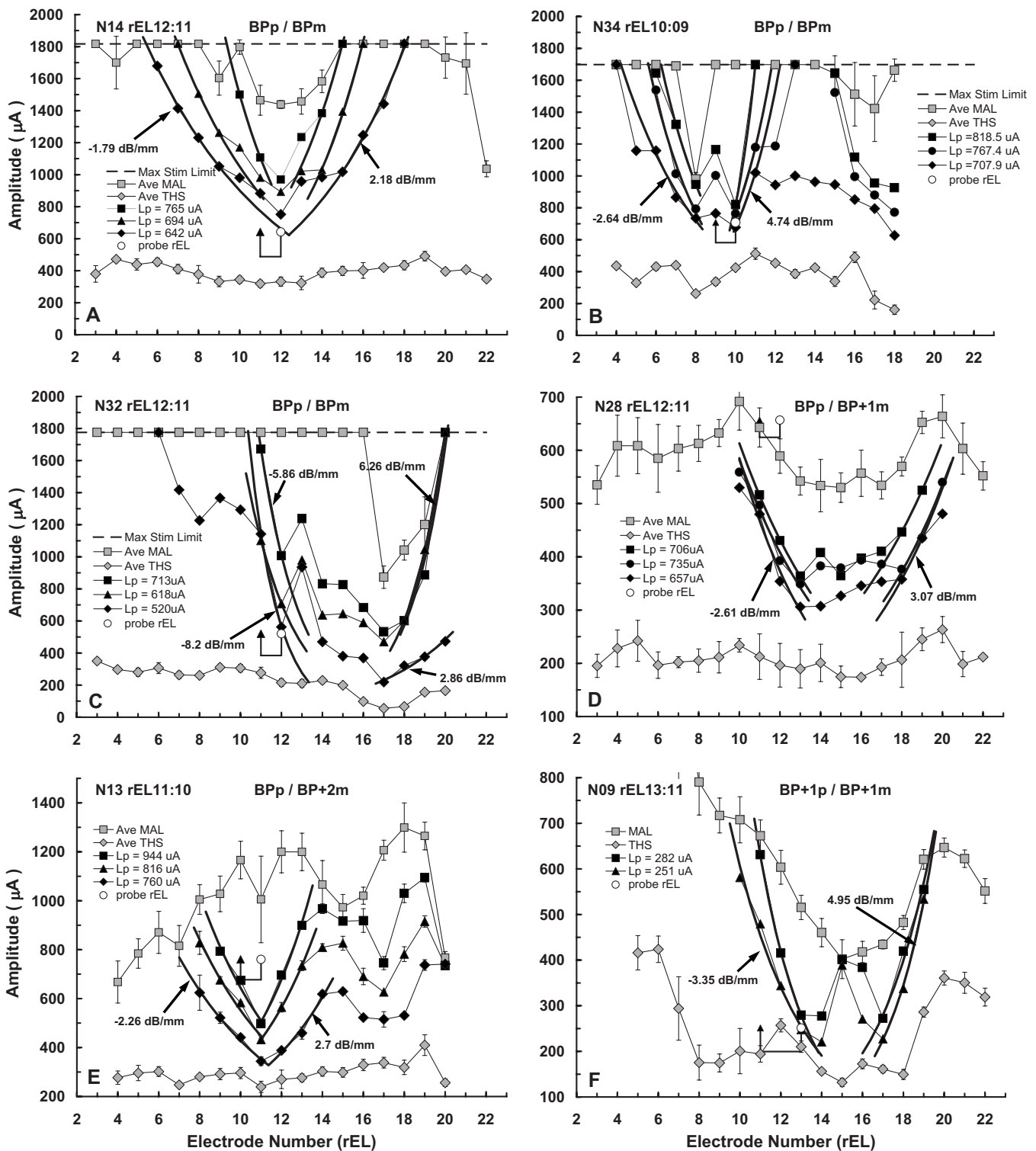


FIG. 4. fmSTCs from six Nucleus-22 cochlear-implant users who were stimulated using a bipolar electrode configuration (BP, BP+1 or BP+2, corresponding to 0.75, 1.5, or 2.25 mm separations between the active and reference electrodes, respectively). Other features of the individual graphs are the same as those described for Fig. 2, except that only the lowest probe level is plotted.

BP+1 probe and a BP+1 masker. Recall that this subject was also stimulated with 125-Hz stimuli, rather than the 500-Hz stimuli used for other subjects. Because bipolar (BP, BP+1, or BP+2) maskers were used for these Nucleus subjects, THSs and MALs for the maskers were considerably higher than those obtained from Clarion subjects using monopolar stimulation. In addition, there was greater variability

across electrodes within an individual for the Nucleus subjects. As in Fig. 3, only the lowest probe level is indicated on each graph. Table III provides the slopes, bandwidths, and tip-shift parameters for the fmSTCs in Fig. 4 from Nucleus subjects.

A wide range of fmSTC characteristics was exhibited by the Nucleus users. Slopes ranged between 1.7 and 8.2

TABLE III. Spatial tuning curve parameters in Nucleus subjects.

Subject probe rEL	Ave Lp (%DR μ A)	Slopes (dB/mm)		Bandwidth (mm)	Tip shift (mm)	Ap/Am (dB)
		Apical	Basal			
N14 rEL12:11	20	-3.52	3.15	1.54	0.82	-2.1
	14	-2.11	3.29	2.72	0.80	-2.2
	9	-1.79	2.18	2.69	0.91	-1.4
N34 rEL10:09	21	-3.87	8.44	1.55	0.09	0.0
	17	-3.84	5.04	1.94	-0.02	0.1
	11	-2.64	4.74	1.50	0.07	0.4
N32 rEL12:11	24	-5.86	6.26	3.79	3.42	-3.0
	17	-5.12	6.27	3.82	3.15	-1.2
	10	-8.20	2.86	3.06	3.16	-0.7
N28 rEL12:11	33	-2.05	2.09	4.53	3.19	5.4
	25	-2.02	1.86	3.83	2.91	4.3
	11	-2.61	2.26	4.06	3.06	5.4
N13 rEL11:10	29	-2.69	3.42	0.56	0.73	5.5
	17	-2.43	3.07	0.61	0.77	5.5
	12	-2.26	2.70	1.16	0.97	6.9
N09 rEL13:11	31	-4.71	4.13	3.36	3.01	0.1
	22	-3.35	4.95	3.10	3.12	0.1
Ave (N)	18.9	-3.48	3.92	2.58	1.77	1.4
Sdev (N)	7.6	1.70	1.81	1.26	1.35	3.3
Min (N)	8.6	-1.79	1.86	0.56	-0.02	-3.0
Max (N)	32.9	-8.20	8.44	4.53	3.42	6.9

dB/mm, and bandwidths ranged between 0.6 and 4.5 mm (not shown in Fig. 4, but given in Table III). In general, these fmSTCs obtained with bipolar stimulation were much sharper and included more irregularities than those obtained from the Clarion subjects with monopolar stimulation. Notice that MALm values varied across electrodes for all of the subjects, and that THSp values also varied across electrodes in a few subjects [especially N09, Fig. 4(F)]. In addition, there were irregularities in masked thresholds within the fmSTC tip regions (between the two slopes) for several subjects (N34, N32, N28, N09). These irregularities could reflect variations in neural survival (Kawano *et al.*, 1998; Saunders *et al.*, 2002; Pfingst and Xu, 2004; Pfingst *et al.*, 2004), nonuniform current pathways resulting from individual variations in cochlear impedances, or peaks and nulls in the current fields produced by the bipolar maskers. The inverted tips demonstrated by these subjects (especially N09) are reminiscent of “split-tip” neural tuning curves described by Kral *et al.* (1998). Kral *et al.* attributed the split tips to peaks and nulls that occur in bipolar current fields.³

Three of the Nucleus subjects (N14, N34, and N13), exhibited fmSTC tips close to the probe electrode in terms of longitudinal distance, suggesting that a functional population of neural elements exists in the region of the probe electrode. However, two of these subjects (N13 and N34), also demonstrated a secondary tip in the basal region of the electrode array. This implies that there is cross-talk between basal and middle regions of the cochlea. One possibility is that stimuli presented on basal electrodes, near the secondary tip, activate fibers of passage originating near the probe electrode as they pass through the modiolus to exit from the cochlea (Frijns *et al.*, 2001).

The remaining three Nucleus subjects (N32, N28, and N09) demonstrated displaced tuning curves, with the fmSTC tips located 2.9–3.4 mm basal to the probe electrode. These three subjects may have better nerve survival in the basal region of the cochlea than in the middle region. However, realistic conclusions about nerve survival (e.g., “dead regions”) must await a more complete evaluation of the displaced spatial tuning in these subjects’ cochleas. This will require the measurement of fmSTCs for additional probe electrodes, both in the basal and apical regions of the electrode array.

Figure 5 summarizes the fmSTC slope parameters from Tables II and III in graphical form. Figure 5(A) shows the slope data for Clarion subjects (monopolar stimulation), and Fig. 5(B) shows the corresponding data for Nucleus subjects (bipolar stimulation). Two key findings can be observed from these data. First, the fmSTC slopes of both Clarion and Nucleus subjects are essentially constant with probe level, for the range of probe levels sampled (approximately 8–33 %DR μ A). Second, the slopes for Nucleus subjects are approximately three times as steep as those for Clarion subjects.

The latter finding is consistent with previous reports that current attenuates two to three times more rapidly for bipolar stimulation than for monopolar stimulation with increasing distance from the source (Black and Clark, 1980; Black *et al.*, 1981, 1983; O’Leary *et al.*, 1985; Hartmann and Klinke, 1990; Kral *et al.*, 1998). That finding is also consistent with most previous studies that employed psychophysical forward masking patterns to examine spread of excitation across the electrode array (Shannon, 1983b; Lim *et al.*, 1989; Boex *et al.*, 2003; Chatterjee *et al.*, 2006). In general, these studies

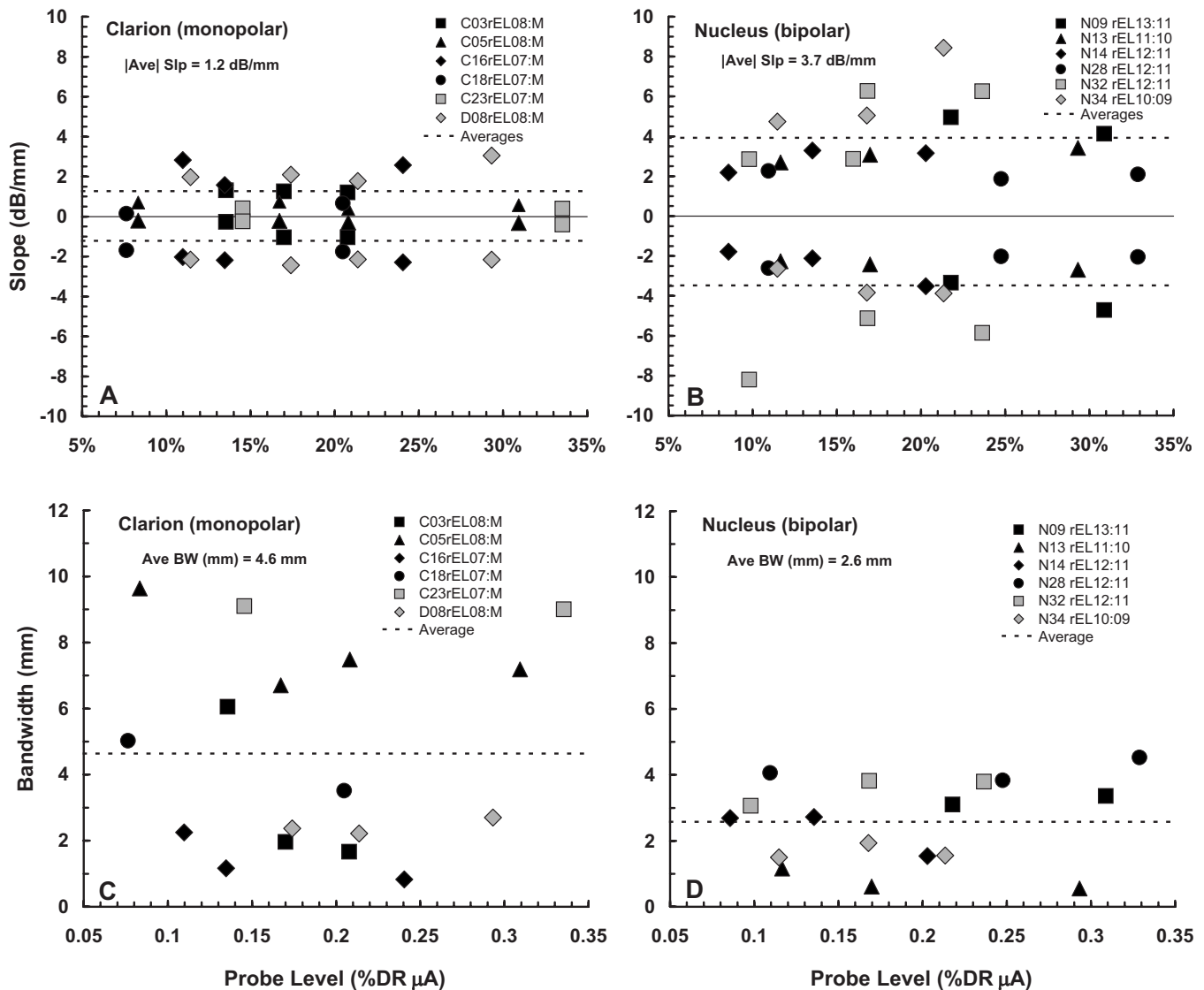


FIG. 5. fmSTC slopes and bandwidths. Slopes (dB/mm) of the fmSTCs obtained from Clarion subjects (A) and Nucleus subjects (B) are shown as a function of probe level, expressed as a percentage of the probe dynamic range in microamperes. In each panel, apical slopes are plotted as negative values and basal slopes are plotted as positive values. Different symbols represent different subjects, as indicated in the legends of each graph, and dashed lines indicate the average slopes for each group. The average of the absolute values (disregarding sign) of both apical and basal slopes is indicated under the heading of each graph. $Q_{1\text{ dB}}$ bandwidths (mm) of fmSTCs obtained from Clarion subjects (C) and Nucleus subjects (D) are shown as a function of probe level, which is expressed as a percentage of the probe dynamic range in μA . Different symbols represent different subjects, as indicated in the legends of each graph. The average $Q_{1\text{ dB}}$ bandwidth for each group is shown by the horizontal dashed line and is given under the heading of each graph.

have found that masking patterns are broader for monopolar stimulation than for bipolar stimulation, but that differences in slopes are not nearly so dramatic as those seen here for spatial tuning curves. An exception to this general finding was reported by [Kwon and van den Honert \(2006\)](#), who found little difference in the spread of forward masking across electrodes for monopolar and bipolar stimulation.

Note from Tables II and III that the absolute variability of slopes is approximately twice as large for the Nucleus (bipolar) subjects (1.75 dB/mm) than for the Clarion (monopolar) subjects (0.9 dB/mm). However, this difference is reduced substantially when the variability is normalized with respect to the mean slope (S.D./mean), leading to values of 0.47 and 0.72, respectively.

Figure 5 also summarizes the bandwidth parameters from Tables II and III. Figure 5(C) shows the bandwidth data

for Clarion subjects (monopolar stimulation), and Fig. 5(D) shows the corresponding data for Nucleus subjects (bipolar stimulation). Again, two key findings are apparent. First, although level effects occur for a few individual subjects (e.g., Clarion subject C03; Nucleus subject N14), there is no systematic effect of probe level on the bandwidths of fmSTCs for subjects in either group. Second, average bandwidths are about twice as large in Clarion (monopolar) subjects as they are in Nucleus (bipolar) subjects, consistent with the slope differences observed in Fig. 5. The absolute variability of fmSTC bandwidths is substantially larger for the Clarion subjects than for the Nucleus subjects. However, similar to the slope estimates, the normalized variability is fairly consistent across the two groups (0.49 and 0.66 for Nucleus and Clarion subjects, respectively).

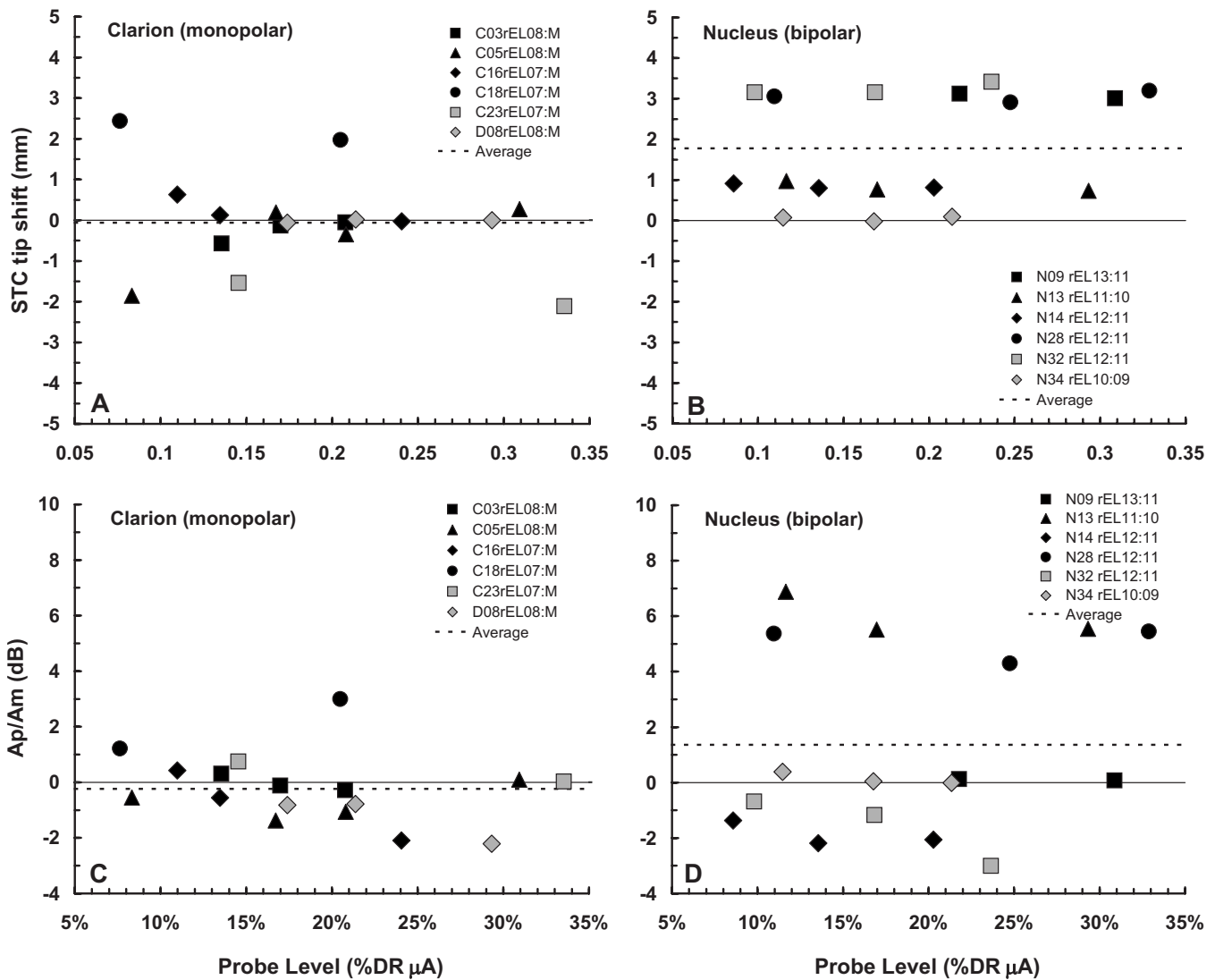


FIG. 6. fmSTC tip shifts and Ap/Am ratios. Mistuning of the fmSTCs obtained from Clarion subjects (A) and Nucleus subjects (B), expressed as the “tip shift” (mm) between the STC tip and the probe electrode, is shown as a function of probe level, which is expressed as a percentage of the probe dynamic range in microamperes. Positive values indicate a tip shift toward the base of the cochlea; negative values indicate a tip shift toward the apex. Different symbols represent different subjects, as indicated in the legends of each graph, and dashed lines indicate the average tip shift for each group. The Ap/Am ratio on the probe electrode from Clarion subjects (C) and Nucleus subjects (D) is shown as a function of probe level, expressed as %DR μ A. The Ap/Am ratio is an indicator of the relative amount of forward masking produced in each subject. It shows the level of the probe relative to the level of the masker at masked threshold, in this case when both the masker and the probe are on the same electrode.

Figure 6 summarizes the tip-shift and Ap/Am ratio data from Tables II and III, using a similar format as Fig. 5. The tip-shift data are shown in Figs. 5(A) and 5(B). Evaluation of the individual subjects’ data within each panel indicates that estimates of tip location are generally unaffected by probe level. Two Clarion subjects (C18, C23) and three Nucleus subjects (N09, N28, N32) showed consistent tip shifts of more than 1 mm. While the two Clarion subjects had tip shifts in opposite directions (one apical and one basal), the three Nucleus subjects all demonstrated tip shifts in the basal direction. There is some evidence of asymmetrical flow of current toward the base of the cochlea in electrical stimulation (Lim *et al.*, 1989), which could be viewed as a possible explanation for the basalward shifts observed among Nucleus subjects. However, it seems unlikely that asym-

metrical current flow could underlie the large tip shifts seen here for some subjects, especially given the low probe levels that were used.

Although it was not discussed earlier, absolute probe thresholds (THSp) varied considerably within the groups of Clarion and Nucleus subjects (Figs. 3 and 4). In particular, several subjects (C18, N13 and, especially, N28) demonstrated absolute probe thresholds that were substantially elevated in comparison to the masked probe threshold on the probe electrode. The last column of Table III summarizes the relation between probe amplitude (Ap) and masker amplitude (Am) at masked threshold, by computing the ratio Ap/Am in decibels when the masker and the probe are on the same electrode. Recall that the amplitude of the masker, at masked threshold represents the amplitude of a 160-ms masker pulse train required to forward mask the 10-ms probe

TABLE IV. Statistical results.

Linear regression analyses [$y=ax+b$, x =probe level (%DR μ A)]						
y	a	b	R^2	F	df	p
Clarion (monopolar)						
Apical slope (dB/mm)	0.00	-1.28	0.00	0.01	15	0.92
Basal slope (dB/mm)	0.01	1.05	0.01	0.15	15	0.71
$Q_{1\text{ dB}}$ bandwidth (mm)	0.00	4.55	0.00	0.00	15	0.96
Tip shift (mm)	-0.03	0.55	0.05	0.71	15	0.41
Ap/Am (tip)	-0.05	0.62	0.08	1.22	15	0.29
Nucleus (bipolar)						
Apical slope (dB/mm)	0.01	-3.65	0.00	0.02	15	0.88
Basal slope (dB/mm)	0.03	3.41	0.01	0.20	15	0.66
$Q_{1\text{ dB}}$ bandwidth (mm)	0.03	1.98	0.04	0.56	15	0.47
Tip shift (mm)	0.05	0.76	0.09	1.49	15	0.24
Ap/Am (tip)	0.08	-0.10	0.03	0.49	15	0.50
T-tests [Clarion monopolar vs Nucleus bipolar]						
	t	df	p			
Apical slope (dB/mm)	3.68	10	0.004			
Basal slope (dB/mm)	-3.79	10	0.004			
$Q_{1\text{ dB}}$ bandwidth (mm)	1.623	10	0.14			
Tip shift (mm)	-2.35	10	0.04			
Ap/Am (tip) ^a	$T=30.0^a$	$n=6,6^a$	0.18			

^aMann-Whitney rank sum test used because equal variance test failed.

pulse train. The Ap/Am ratio varies considerably across subjects (-3 to +7 dB), indicating that the masker stimulus produced different amounts of forward masking for different individuals. These differences in masker effectiveness likely reflect differences in temporal integration across subjects (Donaldson *et al.*, 1997), as well as differences in the rate of recovery from forward masking (Nelson and Donaldson, 2002; Dingemans *et al.*, 2006). Temporal integration is a factor because the probe stimulus is considerably shorter than the masker stimulus and, therefore, has a higher absolute threshold (compare probe thresholds and masker thresholds for the fmSTCs in Figs. 3 and 4). Recovery from forward masking determines the extent to which the masker stimulus shifts the threshold for the probe stimulus at a fixed masker-probe time delay.

Table IV summarizes the statistical results that confirm the above-described findings. Linear regression analyses indicated that there were no significant effects of probe level on any of the fmSTC parameters examined (apical slope, basal slope, bandwidth, tip-shift or Ap/Am ratio). T-tests performed on the average parameter values (collapsed across probe levels) for each subject confirmed that both apical and basal fmSTC slopes were shallower in Nucleus (bipolar) subjects than in Clarion (monopolar) subjects. A t-test performed on the bandwidths did not show a significant difference between groups, even though mean bandwidths were about half as large for the Nucleus (bipolar) subjects as for the Clarion (monopolar) subjects. This can be attributed to the relatively large variability in bandwidths exhibited by the Clarion subjects (Fig. 5). Finally, t-tests showed no significant differences between groups for either the tip-shift or Ap/Am ratio parameters.

B. Normal-hearing and hearing-impaired fmPTCs in acoustic hearing

One goal of this investigation was to compare fmSTC-based measures of spatial selectivity in cochlear implant listeners with previously reported fmPTC-based measures of frequency selectivity in normal-hearing and hearing-impaired acoustic listeners. For this comparison, we used fmPTCs obtained by Nelson (1991) in normal-hearing listeners and listeners with sensorineural hearing loss, which were obtained with a forward-masking procedure similar to that used in the present study. The acoustic maskers were 200-ms (peak duration) tone bursts that forward-masked a 20-ms acoustic tone burst at 1000 Hz. The offset-to-offset delay was 42 ms. Twenty-six normal-hearing listeners and twenty-four hearing-impaired listeners with varying degrees of hearing loss were tested. Example fmPTCs for two probe levels in one normal-hearing listener [Fig. 7(A)] and one hearing-impaired listener [Fig. 7(B)] are shown. Acoustic levels on the ordinate are decibels relative to the threshold at 1000 Hz. Note that the ordinates span a different range of levels for the normal-hearing and hearing-impaired listeners, reflecting the different dynamic ranges available to the two listeners.

Figure 7(A) shows fmPTCs from a normal-hearing listener for two probe levels. Stimulus level is plotted on the ordinate in decibels relative to unmasked threshold at 1000 Hz. For this normal-hearing listener, threshold for the masker was 4.4 dB SPL and threshold for the probe was 12 dB SPL at 1000 Hz. At some of the remote masker frequencies, masker levels up to 105 dB SPL were required to mask the probe tone. The difference between absolute threshold for the masker and the maximum masker levels required to mask the probe reveals a dynamic range of about 100 dB.

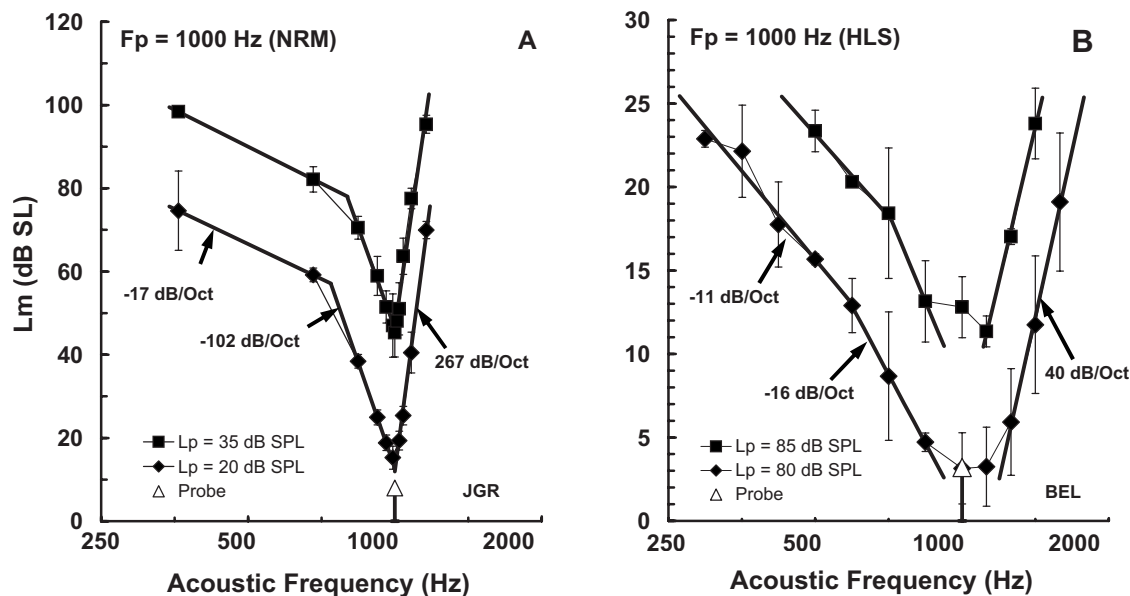


FIG. 7. Forward-masked psychophysical tuning curves (fmPTCs) from acoustic listeners obtained with a procedure comparable to that used to obtain the fmSTCs for the cochlear-implant subjects. (A) fmPTCs from a normal-hearing listener at two probe levels. (B) fmPTCs from a listener with sensorineural hearing loss at two probe levels. The ordinate shows decibels relative to thresholds at the probe frequency (1000 Hz).

The fmPTCs have three segments: a high-frequency (HF) segment with an extremely steep slope (e.g., 267 dB/octave), a low-frequency (LF) segment with a moderately steep slope (e.g., -102 dB/octave), and a “Tail” segment with a relatively flat slope (e.g., -17 dB/octave). Bandwidths measured 10 dB above the fmPTC tip corresponded to approximately 12% of the probe frequency. At the lowest probe level, the bandwidth was 116 Hz, yielding a Q value of 8.6. As probe levels increased, the HF and Tail slopes remained relatively constant, and the LF slope decreased. Consequently, Q values decreased at high probe levels.

Figure 7(B) shows fmPTCs from a listener with sensorineural hearing loss. For this hearing-impaired listener, threshold for the masker was 74 dB SPL and threshold for the probe was 77 dB SPL at 1000 Hz. Maximum masker levels were nearly 100 dB SPL at the lowest masker frequencies. The dynamic range between absolute threshold and the most intense maskers that could be tolerated was less than 25 dB, which is about one-fourth of the dynamic range available to normal-hearing listeners. At the lower probe level (80 dB SPL or 3 dB SL), the fmPTC from this hearing-impaired listener is still characterized by three segments, but the slopes are much more gradual and the bandwidths much wider than for a normal-hearing listener. Specifically, for the lower probe level, the HF slope is 40 dB/octave and the LF slope is -16 dB/octave, both much shallower than for the normal-hearing listener; the Tail slope is -11 dB/octave, which is not much different than for the normal-hearing listener. The bandwidth is 858 Hz (86% of the probe frequency), which corresponds to a Q value of only 1.16. As probe level is increased, the fmPTC parameters change very little.

C. Spatial tuning expressed as tonotopic frequency

In order to make meaningful comparisons between fmSTCs in electric hearing and fmPTCs in acoustic hearing, the

fmSTCs must be displayed using the same frequency scale as that used in acoustic hearing. This requires a transformation between spatial distance along the electrode array and acoustic frequency. Previous research has provided a tonotopic map that relates distance along the basilar membrane to characteristic frequency in an adult human cochlea (Greenwood, 1961, 1990). Using Greenwood’s equation, it is possible to approximate the nominal acoustic frequency region associated with each electrode in a given cochlear-implant listener’s ear, and to replot electrically stimulated fmSTCs in terms of “spatial frequency” (Hertz) instead of spatial distance (millimeters).⁴

Example fmSTCs plotted in terms of spatial frequency are shown in Fig. 8 for data from Nucleus subject N14. Stimulus level is plotted on the ordinate, in decibels relative to the threshold for the probe electrode, as a function of spatial frequency on the abscissa, in Hertz using a logarithmic scale similar to that used in Fig. 7. Tuning curve parameters were calculated for the spatial-frequency fmSTCs using a procedure similar to that used earlier to calculate parameters for the spatial-distance fmSTCs. Specifically, curves were fitted to each fmSTC using a least-squares fitting procedure which related log (microamperes) on the ordinate to log (hertz) on the abscissa. The slopes were expressed in units of decibel/octave. Bandwidths were calculated (in hertz) at a masker level 1 dB above the minimum masker level, and were expressed as Q values (tip frequency divided by bandwidth). These are the same metrics used to describe acoustic tuning curves. The resultant fmSTC parameters, expressed in terms of spatial frequency, are given in Table V for Clarion subjects and Table VI for Nucleus subjects. The slopes in Tables V and VI are expressed in terms of decibels per octave, comparable to slopes of fmPTCs in acoustic hearing.

Absolute slopes for the fmSTCs from listener N14 (Fig. 8) ranged between 8 and 16 dB/octave. Bandwidths ranged

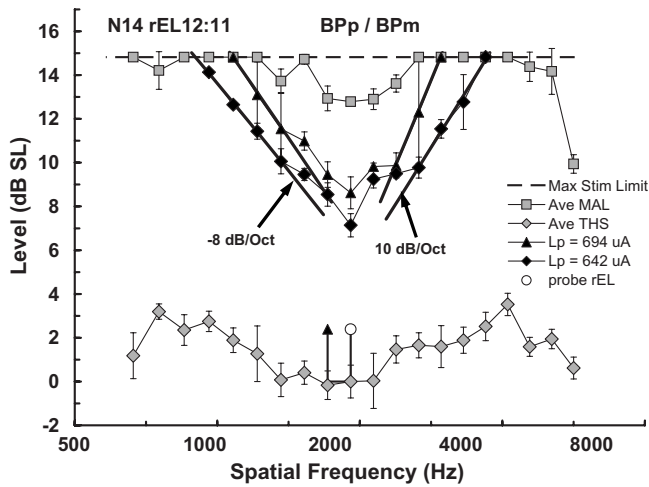


FIG. 8. Forward-masked spatial tuning curves (fmSTCs) from a cochlear implant listener, plotted in terms of spatial frequency calculated from [Greenwood's \(1961\)](#) place-frequency function. The fmSTCs are two of those shown in Fig. 4(A), but for comparison with acoustic fmPTCs, the abscissa has been converted to the spatial frequency corresponding to each electrode, and the ordinate is decibels relative to thresholds on the probe electrode.

between 23% and 40% of the spatial frequency corresponding to the probe electrode, yielding Q values between 4.4 and 2.5. For comparison with acoustic hearing, note that the dynamic range between absolute threshold for a masker stimulus on the probe electrode and the maximum acceptable stimulus level was only 14.8 dB. This dynamic range is less than one-sixth of that available to the normal-hearing listener shown previously. Also note that the low-frequency (apical) side of then fmSTC has only one distinct segment, as compared to the two segments that can be seen in acoustic fmPTCs.

The average tip frequency for fmSTCs was 1536 Hz (range 1105–2347 Hz) for the Clarion subjects and 2650 Hz (range 1838–4298 Hz) for the Nucleus subjects. The differences in average tip frequencies between groups was partially due to the selection of a range of middle electrodes for testing (rEL10 through rEL13 in Nucleus subjects, and rEL07 and rEL08 in Clarion subjects) and partially due to the basalward tip shifts seen in several Nucleus subjects, described earlier. Slopes of the fmSTCs averaged 6 dB/octave for the Clarion subjects and 17 dB/octave for the Nucleus subjects. Average Q values were 2.17 for the Clarion subjects and 3.86 for the Nucleus subjects.

D. Comparisons of tuning in acoustic and electric hearing

Figure 9 compares the tuning characteristics of normal-hearing and hearing-impaired acoustic listeners from [Nelson \(1991\)](#) with the tuning characteristics of the cochlear-implant subjects tested in the present study. Each panel shows a different tuning-curve parameter plotted against dB SPL for the acoustic listeners and percent dynamic range (calculated in microamperes) for the cochlear-implant listeners. Each data point represents a measurement from the tuning curve for an individual listener at a given probe level. Data for one or more probe levels are plotted for each subject.

Figure 9(A) shows that LF slopes decrease with increasing probe level in normal-hearing listeners (closed squares). LF slopes for hearing-impaired ears (closed diamonds and open circles) are similar to those for normal-hearing ears at high probe levels. This is true even for the hearing-impaired ears that exhibit abnormal tuning (open circles). The normal-hearing listeners have much steeper LF slopes than the

TABLE V. Spatial-frequency tuning curve parameters in Clarion subjects.

Subject probe rEL	Ave Lp (%DR μ A)	Slopes (dB/octave)		STCtip (Hz)	Bandwidth (Hz)	Bandwidth (% CF)	Q1 dB (CF/BW)
		Apical	Basal				
C23rEL07:M	34	-1.70	1.87	1184	1767	149.2%	0.67
	15	-1.04	1.91	1294	1798	139.0%	0.72
C05rEL08:M	31	-1.41	2.71	1533	1735	113.2%	0.88
	21	-0.81	1.80	1396	1665	119.3%	0.84
	17	-0.94	3.51	1515	1593	105.1%	0.95
C18rEL07:M	8	-0.89	3.32	1105	1792	162.1%	0.62
	20	-8.01	3.11	2193	1146	52.3%	1.91
C03rEL08:M	8	-7.69	0.68	2347	1767	75.3%	1.33
	21	-4.59	5.60	1459	370	25.4%	3.94
C16rEL07:M	17	-4.63	5.88	1442	431	29.9%	3.34
	14	-1.15	6.19	1348	1286	95.4%	1.05
	24	-10.37	12.02	1629	202	12.4%	8.05
D08rEL08:MP	11	-9.94	7.43	1666	292	17.5%	5.71
	21	-9.31	13.46	1797	606	33.7%	2.96
	29	-9.77	14.38	1375	979	71.2%	1.40
Ave (C)	21	-9.64	8.39	1351	1021	75.6%	1.32
	17	-10.98	9.90	1443	1212	84.0%	1.19
	18.9	-5.46	6.01	1534	1157	80.0%	2.17
Sdev (C)	7.5	4.11	4.31	325	587	47.1%	2.06
Min (C)	7.6	-10.98	0.68	1105	202	12.4%	0.62
Max (C)	33.5	-0.81	14.38	2347	1798	162.1%	8.05

TABLE VI. Spatial-frequency tuning curve parameters in Nucleus subjects.

Subject probe rEL	Ave Lp (%DR μ A)	Slopes (dB/octave)		STCtip (Hz)	Bandwidth (Hz)	Bandwidth (% CF)	Q 1 dB (CF/BW)
		Apical	Basal				
N14 rEL12:11	20	-16.18	14.96	1932	443	22.9%	4.36
	14	-9.46	15.65	1927	784	40.7%	2.46
	9	-7.95	10.47	1959	786	40.1%	2.49
N34 rEL10:09	21	-17.76	39.69	1868	433	23.2%	4.31
	17	-17.52	23.71	1838	532	29.0%	3.45
	11	-12.06	22.29	1863	416	22.3%	4.48
N32 rEL12:11	24	-27.75	30.57	3777	2078	55.0%	1.82
	17	-24.25	30.62	3637	2020	55.5%	1.80
	10	-38.82	10.94	3639	1613	44.3%	2.26
N28 rEL12:11	33	-6.43	8.19	2740	1835	67.0%	1.49
	25	-9.42	9.01	2630	1487	56.5%	1.77
	11	-12.15	10.93	2686	1610	59.9%	1.67
N13 rEL11:10	29	-12.47	16.09	1980	164	8.3%	12.09
	17	-11.20	14.46	1990	181	9.1%	11.01
	12	-10.43	12.77	2052	353	17.2%	5.81
N09 rEL13:11	31	-22.57	20.19	4230	2049	48.4%	2.06
	22	-15.99	24.21	4298	1918	44.6%	2.24
Ave (N)	18.9	-16.02	18.51	2650	1100	37.9%	3.86
Sdev (N)	7.6	8.35	8.91	905	739	18.4%	3.15
Min (N)	8.6	-6.43	8.19	1838	164	8.3%	1.49
Max (N)	32.9	-38.82	39.69	4298	2078	67.0%	12.09

hearing-impaired listeners at low SPLs, where the hearing-impaired listeners cannot hear. The sharp tuning at low SPLs in normal-hearing listeners stems from cochlear processes related to the outer hair cells, which are dysfunctional in the hearing-impaired listeners. The LF (apical) slopes of fmSTCs in cochlear-implant listeners (Clarion=shaded triangles; Nucleus=shaded circles), are substantially shallower than the LF slopes measured in normal-hearing listeners at low probe levels; however, they are roughly equivalent to the LF slopes measured in normal-hearing and hearing-impaired listeners at high probe levels.

Figure 9(B) shows that the HF slope is extremely steep in normal-hearing listeners (closed squares), and in many hearing-impaired listeners (closed diamonds). Some of the hearing-impaired listeners (open circles) exhibited more gradual HF slopes, which led Nelson (1991) to classify them as having abnormal tuning. By comparison, the HF (basal) slopes of most of the cochlear-implant listeners are more gradual. Many of the Nucleus users (shaded circles), who were stimulated in a bipolar electrode configuration, exhibited HF slopes in the same range as the hearing-impaired acoustic listeners with abnormal tuning (open circles). All of the Clarion users (shaded triangles), who were stimulated in a monopolar mode, exhibited HF slopes that were shallower than those for the hearing-impaired listeners with abnormal tuning.

Figure 9(C) shows that the Tail slope is relatively level-independent in normal-hearing and hearing-impaired listeners. The Tail slope presumably reflects tuning in the auditory system without the sharply tuned amplification mechanisms of the normal cochlea. That is, it reflects passive mechanical tuning associated with the traveling wave. Comparisons with

the LF and HF slopes from cochlear-implant listeners reveal that Nucleus listeners (shaded circles), who were stimulated in a bipolar mode, exhibited tuning-curve slopes (either LF or HF slopes) that were similar to Tail slopes in acoustic hearing. Clarion listeners (shaded triangles), who were stimulated in a monopolar mode, exhibited tuning-curve slopes that were shallower than Tail slopes in acoustic hearing.

Figure 9(D) compares bandwidth estimates obtained from acoustic listeners and cochlear-implant listeners expressed as Q values (CF/BW). Q values range from about 10 in the normal-hearing listeners at low probe levels, to about 1 in the normal-hearing and hearing-impaired listeners at very high probe levels. Q values are even smaller in hearing-impaired listeners with abnormal tuning.⁵ The Q values for cochlear-implant listeners fall within the range of those obtained at high probe levels in the acoustic listeners.

The Nelson (1991) data for acoustic listeners were obtained using a probe frequency of 1000 Hz. In contrast, the present data for cochlear-implant listeners varied in terms of the spatial frequency corresponding to the tip of the fmSTC. Tip frequencies ranged between 1105 and 2347 Hz for the Clarion subjects and between 1838 and 4298 Hz for the Nucleus subjects. It is well known in acoustic hearing that tuning becomes sharper with increasing probe frequency (Glasberg and Moore, 1990; Oxenham and Shera, 2003), i.e., Q values increase with probe frequency. Therefore, a fair comparison of the acoustic and cochlear-implant data requires comparison at the same probe frequencies. Fortunately, PTCs have been investigated for a wide range of frequencies in normal-hearing subjects, and an equation has been published that defines changes in Q values with probe

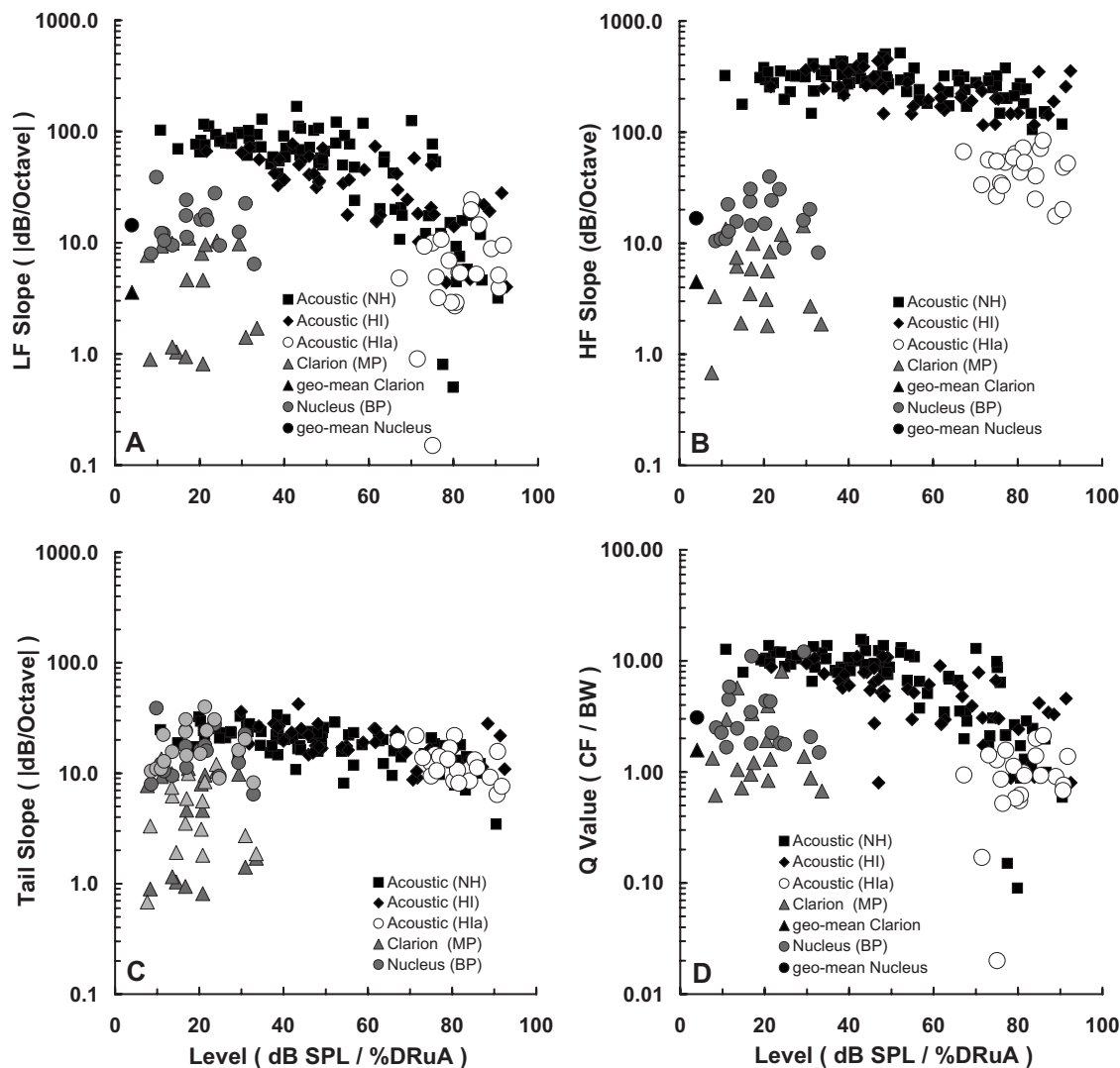


FIG. 9. Tuning characteristics of fmPTCs in normal-hearing and hearing-impaired acoustic listeners, taken from previous work by Nelson (1991), compared with tuning characteristics of fmSTCs obtained from Clarion (monopolar) and Nucleus (bipolar) cochlear implant listeners. Each panel plots a different tuning parameter for three groups of acoustic listeners along with two groups of cochlear-implant listeners. Normal-hearing (NH) acoustic listeners are represented by the black squares; hearing-impaired acoustic listeners with relatively normal tuning (HI) are represented by the black diamonds; hearing-impaired acoustic listeners with abnormal tuning (HIa) are represented by the open circles (abnormal tuning was judged by the HF slope). Cochlear-implant listeners are represented by the shaded circles (Clarion—monopolar) and the shaded triangles (Nucleus—bipolar). The tuning parameters for the acoustic listeners are plotted as a function of the level (dB SPL) of the acoustic probe used to collect the fmPTC. A wide range of probe levels were tested in both normal-hearing and hearing-impaired listeners but, of course, the range was smaller in hearing-impaired listeners. The tuning parameters for the cochlear-implant listeners are plotted as a function of percent dynamic range (%DR μ A) for the probe pulse train. In addition, the geometric means for each group of cochlear-implant subjects are shown by the black circle (Clarion) and black triangle (Nucleus) to the left in (A), (B), and (D). In (C), both the LF slopes (dark-shaded triangles) and HF slopes (light-shaded triangles) of the cochlear implant tuning curves are compared with the Tail slopes (black and open symbols) of the acoustic tuning curves.

frequency (Oxenham and Shera, 2003). Using Eq. (5) from Oxenham and Shera (2003), the average Q values for normal-hearing acoustic listeners can be computed for the mean fmSTC tip frequencies measured here in the Clarion and Nucleus subjects (1536 and 2650 Hz). These values are 12.5 and 14.4, respectively. The average acoustic Q value at the highest fmSTC tip frequency evaluated in our cochlear-implant subjects (4298 Hz) is 16.5. If the acoustic hearing data in Fig. 9(D) were transposed so that the origin of the normal-hearing low-level data were positioned at 16.5 instead of 10, the Q values from the cochlear-implant listeners would still fall within the range of Q values obtained at high probe levels in acoustic listeners. Thus, differences in the tip

frequencies tested in our acoustic (Nelson, 1991) and cochlear-implant subjects do not substantially alter the above-described comparisons.

It is also worth noting that the Q values for acoustic and cochlear-implant subjects were calculated at approximately equal levels within the dynamic range of hearing. Q values for the acoustic listeners were based on the bandwidths of the tuning curves 10 dB above the tip level. This corresponds to approximately 10% of the 100+dB dynamic range available to acoustic listeners. Using the same 10-dB criterion to measure bandwidth in cochlear implant users was not realistic, since their dynamic ranges are roughly 1/10th as large as the normal-hearing acoustic dynamic range. In these cochlear-

implant users, the dynamic ranges for the masking stimuli ranged between 7 and 17 dB, averaging 11.3 dB for the Clarion (monopolar) users and 11.9 dB for the Nucleus (bipolar) users. Bandwidths in these subjects were measured 1 dB above the tip level, which also corresponds to approximately 10% of the average dynamic range.

If one were to calculate fmSTC slopes using the percentage of dynamic range in microamperes (%DR μ A) as the dependent variable, instead of absolute microamperes, the values of the %DR μ A/octave slopes would depend upon the size of the dynamic range and the constancy across electrodes of THS and MAL values. Slopes would become exceptionally steep or gradual when either the THS or the MAL varied dramatically across electrodes and the other variable (MAL or THS) did not (e.g., see N13 and N09 in Fig. 4). An analysis of fmSTC slopes in terms of %DR μ A/octave may prove to be useful when predicting speech recognition through the implant, especially if the independent variable for the fmSTC (frequency in octaves) is recalculated according to the acoustic frequency mapping parameters for each individual implant user. However, at this point in time, there is little certainty about the physiological mechanisms underlying dramatic changes in MAL across electrodes. For this reason, we have chosen to limit our analyses of fmSTC slopes to units of absolute μ A/mm and μ A/octave.

We did, however, compare %DRdB/octave slopes from the normal-hearing and the hearing-impaired acoustic tuning curves in Fig. 7 with %DR μ A/octave slopes from the cochlear-implant spatial tuning curves in Fig. 8 (N14). This comparison indicated that the hearing-impaired and cochlear implant slopes were less steep than the normal-hearing slopes, but the cochlear implant slopes were still within the same range as the hearing-impaired slopes. Thus, the general conclusion remained the same: The cochlear implant and the hearing-impaired tuning curve slopes were similar, and both were shallower than the normal-hearing slopes.

E. Factors influencing STC shapes

Cochlear-implant subjects in the present study demonstrated a wide range of fmSTC shapes. The factor with the strongest apparent influence on STC shapes was the mode of electrode coupling: Clarion subjects stimulated in monopolar mode demonstrated substantially shallower STC slopes (1.2 dB/mm, average for apical and basal slopes) than Nucleus subjects stimulated in bipolar mode (3.7 dB/mm). Average bandwidths were also larger for Clarion subjects (4.7 mm) than for Nucleus subjects (2.6 mm), although there was considerable variability in this parameter among Clarion subjects. Since fmSTC slopes are thought to reflect rates of current spread with spatial distance in the cochlea, the slope difference that we observed between Clarion (monopolar) and Nucleus (bipolar) subjects is most likely attributable to differences in rates of current attenuation associated with the two types of electrode coupling. However, some of the variability across subjects within groups may be related to the position of the electrode array within scala tympani. As described in the following, larger distances between the elec-

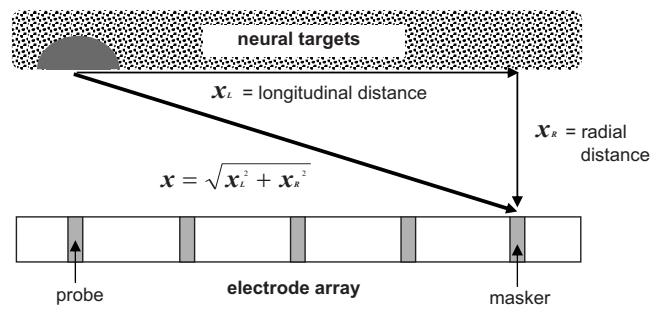


FIG. 10. Schematic demonstrating the spatial relationship between the masker electrode and the neural targets activated by the probe electrode. The horizontal dimension represents longitudinal distance along scala tympani; the vertical dimension represents radial distance between the electrode array and neural targets residing within the modiolus. The dark gray semicircle represents neural targets activated by the low-amplitude probe stimulus.

trode contacts and the residual neurons would be expected to result in fmSTCs with shallower slopes and correspondingly larger bandwidths. Other factors that could potentially contribute to variability across individuals with similar electrode configurations include unique impedance pathways related to individual patterns of neural survival and bone growth in the cochlea (Liang *et al.*, 1999), and variations in the relative electrical resistivities for cochlear bone and fluid. It has been reported that individual differences in cochlear bone-to-fluid resistivity ratios have significant effects on rates of current attenuation in the human cochlea (Whiten and Eddington, 2007); however, to our knowledge, there are no data concerning the range of ratios that exist in human subjects.

To demonstrate the potential influences of stimulation mode and radial distance on the shapes of fmSTCs, we used a simple model to generate hypothetical STCs. Scala tympani was approximated by a tube bordered by residual neurons along one side, as depicted in Fig. 10. The electrode array was displaced from the neural targets by a fixed distance, which corresponds to radial distance in a normal (spiral) cochlea. In Fig. 10, longitudinal distance along the cochlear duct (x_L) is represented in the horizontal dimension, while radial distance (x_R) is represented in the vertical dimension. The linear distance (x) between the masker electrode contact and the neurons closest to the probe electrode was then computed as: $x = \sqrt{x_L^2 + x_R^2}$. x_R was allowed to range from 0 to 3 mm, reflecting the range of physical distances that is likely to exist between an electrode contact and residual nerve fibers or cell bodies within the cochlear modiolus (Cohen *et al.*, 2001; Saunders *et al.*, 2002; Cohen *et al.*, 2006).

The amplitude of current applied to the masker electrode was assumed to decay exponentially with linear distance, following

$$I_p = I_m e^{-x/\lambda}, \quad (1)$$

where I_m is the current amplitude at the masker electrode, I_p is the current amplitude at the probe electrode, x is the distance between the masker and probe electrodes described earlier, and λ is the length constant of current attenuation. This exponential decay function provides a reasonable approximation of current flow, except at locations very close

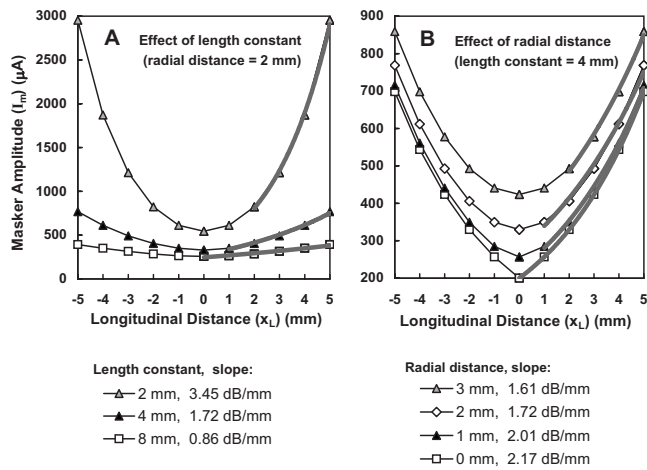


FIG. 11. Hypothetical STCs demonstrating the effect of length constant and radial distance on STC shapes. (A) As the length constant increases from 2 to 8 mm, the tuning curve slope decreases from 3.5 to 0.86 dB/mm. (B) As radial distance increases from 0 to 3 mm, the tip of the STC is elevated and rounded, and the slope is reduced by approximately 25%.

(e.g., <1 mm) to the stimulating electrode (Briaire and Frjns, 2000).

STCs were constructed by computing the level of I_m needed to produce a constant value of I_p , as a function of masker electrode. I_p was fixed arbitrarily at $200 \mu\text{A}$, which approximates the average fmSTC tip levels observed in the present data for monopolar stimulation. Note that altering I_p causes the STC to shift vertically (in overall amplitude), but does not change STC slopes.

Figure 11 shows model STCs demonstrating the effects of stimulation mode and radial distance on STC shapes. In Fig. 11(A), STCs are shown for length constants of 2, 4, and 8 mm, for a fixed radial distance (x_R) of 2 mm. The STCs become progressively broader as the length constant increases from 2 to 8 mm, as expected. Slopes were quantified using the same procedure used for fmSTCs shown in earlier figures; that is, an exponential function was fit to the steepest segments, as indicated by the heavy gray lines. The resultant slopes decreased from 3.5 dB/mm for the 2 mm length constant to 0.86 dB/mm for the 8 mm length constant.

Figure 11(B) demonstrates the effect of radial distance on STC shapes. As radial distance increases, STC slopes become shallower and STCs become more rounded near the tip. In this example, STC slopes decrease approximately 25%, from 2.17 to 1.61 dB/mm, as radial distance increases from 0 to 3 mm. These model STCs were generated using a length constant of 4 mm; however, proportional effects would be observed for other length constants. Radial distance clearly has a much smaller effect on STC slopes than length constant; however, it may account for some portion of the within-group differences in STC slopes and shapes observed in our data.

In order to determine what length constants were most consistent with our average slope data for bipolar and monopolar stimulation (3.7 and 1.2 dB/mm, respectively), theoretical fmSTC slopes were calculated for combinations of length constants ranging from 2 to 10 mm and radial distances ranging from 0 to 3 mm. The resulting slopes are

TABLE VII. Slopes of theoretical fmSTCs (dB/mm), as a function of length constant (mm) and radial distance (mm).

Length constant (mm)	Radial distance			
	0 mm	1 mm	2 mm	3 mm
1	8.69	8.04	6.90	6.46
2	4.34	4.02	3.45	3.23
3	2.90	2.68	2.30	2.15
4	2.17	2.01	1.72	1.61
5	1.74	1.61	1.38	1.29
6	1.45	1.34	1.15	1.08
7	1.24	1.15	0.99	0.92
8	1.09	1.00	0.86	0.81
9	0.97	0.89	0.77	0.72
10	0.87	0.80	0.69	0.65

listed in Table VII. The average monopolar slope measured in the present study (1.2 dB/mm) falls within the range of model slopes (1.08–1.45 dB/mm) generated with a 6-mm length constant, and the average bipolar slope (3.7 dB/mm) falls within the range of model slopes (3.23–4.34) generated with a 2-mm length constant. Thus, our average fmSTC data are consistent with length constants of 2 mm for bipolar stimulation and 6 mm for monopolar stimulation.

Previous studies have estimated current attenuation in the cochlea by measuring current levels directly or by measuring neural responses from the primary auditory nerve or IC as a function of the intracochlear position of the stimulating electrode (see Kral *et al.*, 1998, for a review). Early studies reported length constants of approximately 3 mm for bipolar stimulation and 10 mm for monopolar stimulation (Black and Clark, 1980; Black *et al.*, 1981, 1983; O'Leary *et al.*, 1985). More recent studies which measured primary auditory nerve responses in cat as a function of electrode position have reported attenuation slopes of about 8 dB/mm for bipolar stimulation and 3 dB/mm for monopolar stimulation (Hartmann and Klinke, 1990; Kral *et al.*, 1998). These slopes correspond to length constants of 1 and 3 mm, respectively. Thus, although there is a consistent ratio of monopolar-to-bipolar length constants (~ 3) across studies, the absolute length constants reported in previous studies vary threefold, presumably due to differences in the methodologies employed and species examined (Kral *et al.*, 1998). The average length constants derived from the present fmSTC data fall within the broad range of length constants reported previously. Specifically, our average length constant of 2 mm for bipolar stimulation falls within the range of length constants previously reported for bipolar stimulation (1–3 mm), and our average length constant for monopolar stimulation (6 mm) falls within the range of length constants previously reported for monopolar stimulation (3–10 mm). In addition, our data exhibit a similar ratio of monopolar-to-bipolar length constants (~ 3) as that described in earlier studies.

F. Implications for speech recognition

Given that a primary goal of cochlear implantation is to facilitate speech recognition, it is relevant to consider the

potential relationship between fmSTC parameters, such as those measured in the present study, and speech recognition in individual cochlear implant users. Previous studies have shown that implant users vary widely in their ability to perform various spectral-resolution tasks, and that performance on such tasks may predict speech recognition ability, in general, or the perception of spectral speech cues, in particular (Dorman *et al.*, 1990a, b; Nelson *et al.*, 1995; Dorman *et al.*, 1996; Donaldson and Nelson, 2000; Henry *et al.*, 2000, 2005; Won *et al.*, 2007).

Some of the strongest relations between psychophysical and speech tasks have been observed when both the psychophysical and speech stimuli are presented through the speech processor (Dorman *et al.*, 1990a, b; 1996; Henry *et al.*, 2005; Won *et al.*, 2007). Under those conditions, both tasks are limited by the sum total of constraints to spectral resolution existing for a given individual, which include constraints imposed by the speech processor (compression and basalward shifting of the frequency-place map; analysis bandwidths; filter slopes), constraints associated with the electrode array (spacing between electrode contacts; position of the electrode array within the cochlear duct), and constraints related to the cochlear status of the individual (degree and pattern of auditory nerve survival; bone growth; other factors that influence current pathways).

On the other hand, the fmSTC parameters reported here do not reflect constraints imposed by the speech processor or constraints associated with the electrode array. Instead, they reflect physiological limitations to spatial resolution at the level of the cochlea or above: rates of current attenuation (fmSTC slopes and bandwidths) and distortions in the tonotopic map due to “holes” in neural survival and aberrant current pathways (fmSTC tip locations). Thus, for a given individual and stimulation mode, fmSTC parameters can be considered to reflect the “hard” limits of spatial resolution—those that cannot be readily overcome by improving spatial resolution at the level of the speech processor and/or the electrode array.

Because fmSTC parameters do not reflect limitations to spatial resolution imposed by the speech processor or electrode array, we do not necessarily expect them to correlate strongly with measures of speech recognition obtained through the speech processor. Furthermore, any comparisons between STC parameters and speech recognition should evaluate fmSTCs from multiple probe electrodes per subject. The present study reports fmSTC parameters for only a single electrode near the center of each subject’s electrode array. Thus, the current data are too limited to allow meaningful comparisons to speech recognition scores.

Some of the factors that limit spatial resolution by cochlear implant users, notably those associated with the speech processor and electrode array, can be mitigated by improvements in technology. For example, deeper insertion of electrode arrays allows for less compression of the basic frequency-to-place map (Baskent and Shannon, 2003, 2005; Gani *et al.*, 2007). Similarly, the implementation of current steering in speech processing strategies can potentially reduce limitations related to fixed electrode locations by allowing current peaks to be “steered” to varying locations be-

tween pairs of adjacent electrodes (McDermott and McKay, 1994; Busby and Plant, 2005; Donaldson *et al.*, 2005; Kwon and van den Honert, 2006; Firszt *et al.*, 2007; Koch *et al.*, 2007). However, little has been done thus far to address underlying irregularities in neural survival and aberrant current pathways, which may severely degrade the transmission of spectral information for some CI listeners (Shannon *et al.*, 2001). The development of strategies to compensate for such irregularities will require that “electrotopic” maps be constructed for individual ears. This can be accomplished by analyzing fmSTCs for probe electrodes spanning the entire implanted array, since regions of poor or absent neural survival should produce fmSTCs with shifted or broadened tips. In this way, fmSTCs may prove to be particularly useful for developing remapping strategies for enhancing spectral resolution in individual cochlear implant recipients.

IV. SUMMARY AND CONCLUSIONS

fmSTCs were obtained at several probe levels, for each of six Clarion cochlear implant users stimulated in a monopolar electrode configuration, and for each of six Nucleus cochlear implant users stimulated in a bipolar electrode configuration. Tuning-curve characteristics were calculated for each of the spatial tuning curves and were compared with characteristics of fmPTCs obtained previously in normal-hearing listeners and listeners with sensorineural hearing loss (Nelson, 1991). Analyses led to the following key findings and conclusions:

- (1) fmSTCs measured in cochlear implant users can be characterized by apical and basal slopes (dB/mm) and by bandwidths (mm) measured 1 dB above the tuning-curve tip.
- (2) Apical and basal slopes of fmSTCs are not significantly different from each other, i.e., spatial tuning curves are relatively symmetric for cochlear implant listeners.
- (3) Slopes of fmSTCs are relatively independent of probe level for probe levels between 8% and 33% of the dynamic range of the probe stimulus. This finding is consistent with a linear growth of response in electric hearing. It contrasts with the nonlinear growth of response in normal acoustic hearing that is associated with a progressive decrease in tuning sharpness with stimulus level.
- (4) Slopes of fmSTCs were steeper for subjects stimulated with a bipolar electrode configuration (avg=3.7 dB/mm) than for subjects stimulated with a monopolar electrode configuration (avg=1.2 dB/mm). This primarily reflects differences in the rates of current attenuation for monopolar versus bipolar stimulation. The present data are consistent with length constants of 2 mm for bipolar stimulation and 6 mm for monopolar stimulation. These values fall within the broad range reported in previous studies and, similar to earlier studies, indicate that length constants for monopolar stimulation are approximately three times greater than those for bipolar stimulation. Additional within-subjects research is needed to more precisely define the effects of electrode configuration on fmSTC slopes.

- (5) Bandwidths of fmSTCs measured 1 dB above the STC tip were not significantly different ($p=0.08$) for bipolar subjects and monopolar subjects, even though the average bandwidth for monopolar subjects (4.7 mm) was substantially larger than the average bandwidth for bipolar subjects (2.6 mm). A within-subjects investigation of electrode configuration could eliminate between-subjects variance and potentially reveal a significant effect.
- (6) Some of the individual variability in fmSTC slopes and bandwidths among cochlear implant users with the same device may reflect differences in the radial position of the electrode array within scala tympani.
- (7) Irregularities near the tips of fmSTCs were more common in bipolar subjects than in monopolar subjects. Such irregularities may be due to the peaks and nulls of current fields associated with the bipolar maskers.
- (8) fmSTCs converted to frequency coordinates, by calculating the spatial frequency corresponding to each electrode using a tonotopic place-frequency function (Greenwood, 1961), yield Apical and Basal slopes of fmSTCs that are similar to the Tail slopes of tuning curves measured in acoustic listeners. Consistent with this, bandwidths of fmSTCs are similar to those measured in acoustic listeners at high stimulus levels: The range of Q values in electric hearing overlapped the range of Q values seen at high levels in normal-hearing and hearing-impaired acoustic listeners.
- (9) Taken together, the above-noted findings indicate that cochlear implant users have roughly the same broad spatial frequency resolution at low to moderate stimulus levels that normal-hearing and hearing-impaired acoustic listeners have at high stimulus levels. This relationship is coincidental, since spatial resolution in cochlear implant listeners is governed by different factors (current attenuation rate, radial electrode position, neural survival, and current pathways) than the factors that govern sharpness of tuning in acoustic hearing (active and passive cochlear mechanics). However, it does indicate that the typical cochlear implant user can perform spectral resolution tasks under direct electrical stimulation as well as normal-hearing and hearing-impaired acoustic listeners can perform similar tasks at high sound levels. Thus, constraints imposed by the speech processor and the electrode array, rather than the underlying spatial tuning characteristics, may be the primary factors limiting speech recognition for many cochlear implant users.
- (10) fmSTC obtained from multiple electrodes in an individual cochlear implant user may identify regions of poor or absent neural survival. This knowledge may prove useful for developing remapping strategies to improve implant performance.

ACKNOWLEDGMENTS

This work was supported by NIDCD Grant No. R01-DC006699 and by the Lions 5M International Hearing Foundation. John Van Essen converted Robert Shannon's computer software into the C language and made modifications to that software for testing Nucleus subjects. Cochlear Cor-

poration provided Nucleus subjects' calibration tables. Advanced Bionics Corporation provided the research interface used for testing Clarion subjects, and Eric Javel developed the experimental software to control that interface. The authors would like to extend special thanks to the subjects who participated in this work, and to Andrew Oxenham, Bob Shannon, and an anonymous reviewer, who made valuable suggestions during the review of this manuscript.

¹It should be noted here that a between-subjects design, using subjects with two different types of processors, is not optimal for demonstrating differences due to electrode configuration. However, at the time this research was carried out, it was not possible to implement both monopolar and bipolar stimulation on the same subjects, using the subjects that were available to us. Therefore, we report here the results from a group of Clarion C-I and C-II subjects stimulated in monopolar mode and a group of Nucleus N-22 subjects stimulated in bipolar mode, with the caveat that differences across subjects and processors could influence our group comparisons of monopolar and bipolar electrode configuration.

²Although BP+1 and BP+2 maskers may result in broader tuning than BP maskers, some subjects could not achieve adequate loudness growth with BP probes or adequate forward masking with BP maskers to permit measurement of fmSTCs using a BP/BP configuration. Thus, the present results reflect the spatial tuning available to each subject using the same electrode configuration used in their clinical map.

³The split tip is particularly obvious for N09. It seems unlikely that this is related to the slower pulse rates used for this subject; however, it may be related to the use of a wider bipolar mode (BP+1) for the probe stimulus. Note that the slopes and bandwidths for N09 are not substantially different from the other Nucleus subjects, despite the differences in stimulation rate and electrode configuration.

⁴The term spatial frequency is used here to indicate the acoustic frequency associated with a particular spatial distance along the cochlear duct. It is intended only as an *approximation* of the acoustic frequency previously associated with a particular place. Individual differences in cochlear length or errors in our estimates of insertion depth could have significant effects on our place-to-frequency estimates.

⁵The Q values obtained from normal-hearing listeners at the lowest probe levels compare favorably with the average Q_{ERB} value of 9 obtained using two forward maskers, one above and one below a 1000 Hz probe (Oxenham and Shera, 2003).

- Baskent, D., and Shannon, R. V. (2003). "Speech recognition under conditions of frequency-place compression and expansion," *J. Acoust. Soc. Am.* **113**, 2064–2076.
- Baskent, D., and Shannon, R. V. (2005). "Interactions between cochlear implant electrode insertion depth and frequency-place mapping," *J. Acoust. Soc. Am.* **117**, 1405–1416.
- Bierer, J. A. (2007). "Threshold and channel interaction in cochlear implant users: evaluation of the tripolar electrode configuration," *J. Acoust. Soc. Am.* **121**, 1642–1653.
- Black, R. C., and Clark, G. M. (1980). "Differential electrical excitation of the auditory nerve," *J. Acoust. Soc. Am.* **67**, 868–874.
- Black, R. C., Clark, G. M., and Patrick, J. F. (1981). "Current distribution measurement within the human cochlea," *IEEE Trans. Biomed. Eng.* **28**, 721–724.
- Black, R. C., Clark, G. M., Tong, Y. C., and Patrick, J. F. (1983). "Current distribution in cochlear stimulation," *Ann. N.Y. Acad. Sci.* **405**, 137–145.
- Boex, C., Kos, M. I., and Pelizzone, M. (2003). "Forward masking in different cochlear implant systems," *J. Acoust. Soc. Am.* **114**, 2058–2065.
- Briaire, J. J., and Frijns, J. H. M. (2000). "Field patterns in a 3D tapered spiral model of the electrically stimulated cochlea," *Hear. Res.* **148**, 18–30.
- Busby, P. A., and Plant, K. L. (2005). "Dual electrode stimulation using the Nucleus CI24RE cochlear implant: electrode impedance and pitch ranking studies," *Ear Hear.* **26**, 504–511.
- Chatterjee, M. (1999). "Temporal mechanisms underlying recovery from forward masking in multielectrode implant listeners," *J. Acoust. Soc. Am.* **105**, 1853–1863.
- Chatterjee, M., Galvin, J. J., Fu, Q. J., and Shannon, R. V. (2006). "Effects of stimulation mode, level and location on forward-masked excitation pat-

- terns in cochlear implant patients," *J. Assoc. Res. Otolaryngol.* **7**, 15–26.
- Chatterjee, M., and Shannon, R. V. (1998). "Forward masked excitation patterns in multielectrode electrical stimulation," *J. Acoust. Soc. Am.* **103**, 2565–2572.
- Cohen, L. T., Richardson, L. M., Saunders, E., and Cowan, R. (2003). "Spatial spread of neural excitation in cochlear implant recipients: comparison of improved ECAP method and psychophysical forward masking," *Hear. Res.* **179**, 72–87.
- Cohen, L. T., Saunders, E., and Clark, G. M. (2001). "Psychophysics of a peri-modiolar cochlear implant electrode array," *Hear. Res.* **155**, 63–81.
- Cohen, L. T., Saunders, E., Knight, M. R., and Cowan, R. S. C. (2006). "Psychophysical measures in patients fitted with Contour (TM) and straight nucleus electrode arrays," *Hear. Res.* **212**, 160–175.
- Collins, L. M., and Throckmorton, C. S. (1998). "Investigation of the relationship between psychophysical measures of channel interaction and perceptual structure in subjects with cochlear implants," *Assoc. Res. Otolaryngol. Abstracts*, #872, St. Petersburg, FL.
- Dingemans, J. G., Frijns, J. H. M., and Briare, J. J. (2006). "Psychophysical assessment of spatial spread of excitation in electrical hearing and single and dual electrode contact maskers," *Ear Hear.* **27**, 645–657.
- Donaldson, G. S., Krefth, H. A., and Litvak, L. (2005). "Place-pitch discrimination of single- versus dual-electrode stimuli by cochlear implant users," *J. Acoust. Soc. Am.* **118**, 623–626.
- Donaldson, G. S., and Nelson, D. A. (2000). "Place-pitch sensitivity and its relation to consonant recognition by cochlear implant listeners using the MPEAK and SPEAK speech processing strategies," *J. Acoust. Soc. Am.* **107**, 1645–1658.
- Donaldson, G. S., Viemeister, N. F., and Nelson, D. A. (1997). "Psychometric functions and temporal integration in electrical hearing," *J. Acoust. Soc. Am.* **101**, 3706–3721.
- Dorman, M. F., Dankowski, K., McCandless, G., Parkin, J. L., and Smith, L. (1990a). "Longitudinal changes in word recognition by patients who use the Ineraid cochlear implant," *Ear Hear.* **11**, 455–459.
- Dorman, M. F., Smith, L., McCandless, G., Dunnivant, G., Parkin, J., and Dankowski, K. (1990b). "Pitch scaling and speech understanding by patients who use the Ineraid cochlear implant," *Ear Hear.* **11**, 310–315.
- Dorman, M. F., Smith, L. M., Smith, M., and Parkin, J. L. (1996). "Frequency discrimination and speech recognition by patients who use the Ineraid and continuous interleaved sampling cochlear-implant signal processors," *J. Acoust. Soc. Am.* **99**, 1174–1184.
- Firszt, J. B., Koch, D. B., Downing, M., and Litvak, L. (2007). "Current steering creates additional pitch percepts in adult cochlear implant recipients," *Otol. Neurotol.* **28**, 629–636.
- Frijns, J. H., Briare, J. J., de Laat, J. A., and Grote, J. J. (2002). "Initial evaluation of the Clarion CII cochlear implant: speech perception and neural response imaging," *Ear Hear.* **23**, 184–197.
- Frijns, J. H. M., Briare, J. J., and Grote, J. J. (2001). "The importance of human cochlear anatomy for the results of modiolus-hugging multichannel cochlear implants," *Otol. Neurotol.* **22**, 340–349.
- Fu, Q. J., Chatterjee, M., Shannon, R. V., and Zeng, F. G. (1997). "Comparison of electrode interaction measures in multichannel cochlear implants," *Assoc. Res. Otolaryngol. Abstracts*, #305, St. Petersburg, FL.
- Gani, M., Valentini, G., Sigrist, A., Kos, M. I., and Boex, C. (2007). "Implications of deep electrode insertion on cochlear implant fitting," *J. Assoc. Res. Otolaryngol.* **8**, 69–83.
- Glasberg, B. R., and Moore, B. C. J. (1990). "Derivation of auditory filter shapes from notched-noise data," *Hear. Res.* **47**, 103–138.
- Greenwood, D. D. (1990). "A cochlear frequency-position function for several species—29 years later," *J. Acoust. Soc. Am.* **87**, 2592–2605.
- Greenwood, D. D. (1961). "Critical bandwidth and the frequency coordinates of the basilar membrane," *J. Acoust. Soc. Am.* **33**, 1344–1356.
- Hartmann, R., and Klinke, R. (1990). "Impulse patterns of auditory nerve fibres to extra and intracochlear electrical stimulation," *Acta Oto-Laryngol., Suppl.* **469**, 128–134.
- Henry, B. A., McKay, C. M., McDermott, H. J., and Clark, G. M. (2000). "The relationship between speech perception and electrode discrimination in cochlear implantees," *J. Acoust. Soc. Am.* **108**, 1269–1280.
- Henry, B. A., Turner, C. W., and Behrens, A. (2005). "Spectral peak resolution and speech recognition in quiet: normal hearing, hearing impaired, and cochlear implant listeners," *J. Acoust. Soc. Am.* **118**, 1111–1121.
- Hinojosa, R., and Lindsay, J. R. (1980). "Profound deafness: Associated sensory and neural degeneration," *Arch. Otolaryngol.* **106**, 193–209.
- Hughes, M., Vander Werff, K. R., Brown, C. J., Abbas, P. J., Kelsay, M. R., Teagle, H. F. B., and Lowder, M. (2001). "A longitudinal study of electrode impedance, the electrically evoked compound action potential, and behavioral measures in Nucleus 24 cochlear implant users," *Ear Hear.* **22**, 471–486.
- Jolly, C. N. (1998). "Breakthrough in perimodiolar concepts," presented at the Seventh Symposium on Cochlear Implants in Children, Iowa City (unpublished).
- Jolly, C. N., Spelman, F. A., and Clopton, B. M. (1996). "Quadrupolar stimulation for cochlear prostheses: Modeling and experimental data," *IEEE Trans. Biomed. Eng.* **43**, 857–865.
- Kawano, A., Seldon, H. L., Clark, G. M., Ramsden, R. T., and Raine, C. H. (1998). "Intracochlear factors contributing to psychophysical percepts following cochlear implantation," *Acta Oto-Laryngol.* **118**, 313–326.
- Kessler, D. K. (1999). "The CLARION multi-strategy cochlear implant," *Ann. Otol. Rhinol. Laryngol. Suppl.* **177**, 8–16.
- Koch, D. B., Downing, M., Osberger, M. J., and Litvak, L. (2007). "Using current steering to increase spectral resolution in CII and HiRes 90K users," *Ear Hear.* **28**, 38S–41S.
- Kral, A., Hartmann, R., Mortazavi, D., and Klinke, R. (1998). "Spatial resolution of cochlear implants: the electrical field and excitation of auditory afferents," *Hear. Res.* **121**, 11–28.
- Kwon, B. J., and van den Honert, C. (2006). "Effect of electrode configuration on psychophysical forward masking in cochlear implant listeners," *J. Acoust. Soc. Am.* **119**, 2994–3002.
- Levitt, H. (1971). "Transformed up-down methods in psychoacoustics," *J. Acoust. Soc. Am.* **49**, 467–477.
- Liang, D. M., Lusted, H. S., and White, R. L. (1999). "The nerve-electrode interface of the cochlear implant: Current spread," *IEEE Trans. Biomed. Eng.* **46**, 35–43.
- Lim, H. H., Tong, Y. C., and Clark, G. M. (1989). "Forward masking patterns produced by intracochlear electrical stimulation of one and two electrode pairs in the human cochlea," *J. Acoust. Soc. Am.* **86**, 971–979.
- McDermott, H. J., and McKay, C. M. (1994). "Pitch ranking with nonsimultaneous dual-electrode electrical stimulation of the cochlea," *J. Acoust. Soc. Am.* **96**, 155–162.
- Moore, B. C. J. (2001). "Dead regions in the cochlea: diagnosis, perceptual consequences, and implications for the fitting of hearing aids," *Trends Amplif. S.* **1**, 1–34.
- Moore, B. C. J., and Alcantara, J. I. (2001). "The use of psychophysical tuning curves to explore dead regions in the cochlea," *Ear Hear.* **22**, 268–278.
- Moore, B. C. J., Huss, M., Vickers, D. A., Glasberg, B. R., and Alcantara, J. I. (2000). "A test for the diagnosis of dead regions in the cochlea," *Braz. J. Phys.* **34**, 205–224.
- Morris, D. J., and Pfingst, B. E. (2000). "Effects of electrode configuration and stimulus level on rate and level discrimination with cochlear implants," *J. Assoc. Res. Otolaryngol.* **1**, 211–223.
- Nadol, J. B., Shia, J. Y., Burgess, B. J., Ketten, D. R., Eddington, D. K., Gantz, B. J., Kos, I., Montandon, P., Coker, N. J., Roland, J. T., and Shallop, J. K. (2001). "Histopathology of cochlear implants in the human," *Ann. Otol. Rhinol. Laryngol.* **110**, 883–891.
- Nelson, D. A. (1991). "High-level psychophysical tuning curves: Forward masking in normal-hearing and hearing-impaired listeners," *J. Speech Hear. Res.* **34**, 1233–1249.
- Nelson, D. A., and Donaldson, G. S. (2002). "Psychophysical recovery from pulse-train forward masking in electric hearing," *J. Acoust. Soc. Am.* **112**, 2932–2947.
- Nelson, D. A., and Freyman, R. L. (1984). "Broadened forward-masked tuning curves from intense masking tones: delay-time and probe-level manipulations," *J. Acoust. Soc. Am.* **75**, 1570–1577.
- Nelson, D. A., and Schroder, A. C. (2004). "Peripheral compression as a function of stimulus level and frequency region in normal-hearing listeners," *J. Acoust. Soc. Am.* **115**, 2221–2233.
- Nelson, D. A., Schroder, A. C., and Wojtczak, M. (2001). "A new procedure for measuring peripheral compression in normal-hearing and hearing-impaired listeners," *J. Acoust. Soc. Am.* **110**, 2045–2064.
- Nelson, D. A., Van Tasell, D. J., Schroder, A. C., Soli, S., and Levine, S. (1995). "Electrode ranking of "place pitch" and speech recognition in electrical hearing," *J. Acoust. Soc. Am.* **98**, 1987–1999.
- O'Leary, S. J., Black, R. C., and Clark, G. M. (1985). "Current distribution in the cat cochlea: A modelling and electrophysiological study," *Hear. Res.* **18**, 273–281.
- Oxenham, A. J., and Shera, C. A. (2003). "Estimates of human cochlear tuning at low levels using forward and simultaneous masking," *J. Assoc. Res. Otolaryngol.* **4**, 541–554.

- Patrick, J. F., and Clark, G. M. (1991). "The nucleus 22-channel cochlear implant system," *Ear Hear.* **12**, Suppl., 3S–9S.
- Pfingst, B. E., and Xu, L. (2004). "Across-site variation in detection thresholds and maximum comfortable loudness levels for cochlear implants," *J. Assoc. Res. Otolaryngol.* **5**, 11–24.
- Pfingst, B. E., Xu, L., and Thompson, C. S. (2004). "Across-site threshold variation in cochlear implants: Relation to speech recognition," *Audiol. Neuro-Otol.* **9**, 341–352.
- Saunders, E., Cohen, L., Aschendorff, A., Shapiro, W., Knight, M., Stecker, M., Richter, B., Waltzman, S., Tykocinski, M., Roland, T., Laszig, R., and Cowan, R. (2002). "Threshold, comfortable level and impedance changes as a function of electrode-modiolar distance," *Ear Hear.* **23**, 28S–40S.
- Schindler, R. A., and Kessler, D. K. (1993). "Clarion cochlear implant: phase I investigation results," *Am. J. Otol.* **14**, 263–272.
- Shannon, R. V. (1983a). "Multichannel electrical stimulation of the auditory nerve in man. I. Basic psychophysics," *Hear. Res.* **11**, 157–189.
- Shannon, R. V. (1983b). "Multichannel electrical stimulation of the auditory nerve in man. II. Channel interaction," *Hear. Res.* **12**, 1–16.
- Shannon, R. V. (1986). "Temporal processing in cochlear implants," in *Sensorineural Hearing Loss: Mechanisms, Diagnosis and Treatment—The Reger Conference*, edited by M. J. Collins, T. J. Glatke, and L. A. Harker, pp. 349–367.
- Shannon, R. V. (1990a). "Forward masking in patients with cochlear implants," *J. Acoust. Soc. Am.* **88**, 741–744.
- Shannon, R. V., Adams, D. D., Ferrel, R. L., Palumbo, R. L., and Grandgenett, M. (1990). "A computer interface for psychophysical and speech research with the Nucleus cochlear implant," *J. Acoust. Soc. Am.* **87**, 905–907.
- Shannon, R. V., Galvin, J. J., and Baskent, D. (2001). "Holes in hearing," *J. Assoc. Res. Otolaryngol.* **3**, 185–199.
- Shepherd, R. K., Matsushima, J., Martin, R. L., and Clark, G. M. (1994). "Cochlear pathology following chronic electrical stimulation of the auditory nerve: II Deafened kittens," *Hear. Res.* **81**, 150–166.
- Skinner, M. W., Ketten, D. R., Holden, L. K., Harding, G. W., Smith, P. G., Gates, G. A., Neely, J. G., Kletzker, G. R., Brunsten, B., and Blocker, B. (2002). "CT-Derived estimation of cochlear morphology and electrode array position in relation to word recognition in Nucleus-22 recipients," *J. Assoc. Res. Otolaryngol.* **3**, 332–350.
- Spelman, F. A., Clopton, B. M., and Pfingst, B. E. (1982). "Tissue impedance and current flow in the implanted ear; implications for the cochlear prosthesis," *Ann. Otol. Rhinol. Laryngol.* **91**, 1–8.
- Spoendlin, H., and Schrott, A. (1988). "The spiral ganglion and the innervation of the human Organ of Corti," *Acta Oto-Laryngol.* **105**, 403–410.
- Whiten, D. M., and Eddington, D. K. (2007). "Validating patient-specific electro-anatomical models: Empirically measured and model-predicted evoked potentials and EFI data from the same individual," presented at the 2007 Conference on Implantable Auditory Prostheses, Lake Tahoe, CA (unpublished).
- Wilson, B. S., Lawson, D. T., Zerbi, M., and Finley, C. C. (1994). "Recent developments with the CIS Strategies," in *Advances in Cochlear Implants, Proceedings Third International Cochlear Implant Conference (Innsbruck, Austria, April 1993)*, edited by I. J. Hochmair-Desoyer and E. S. Hochmair (Manz, Wien), pp. 103–112.
- Won, J. H., Drennan, W. R., and Rubinstein, J. T. (2007). "Spectral-ripple resolution correlates with speech reception in noise in cochlear implant users," *J. Assoc. Res. Otolaryngol.* **8**, 384–392.
- Zappia, J. J., Niparko, J. K., Oviatt, D. L., Kemink, J. L., and Altschuler, R. A. (1991). "Evaluation of the temporal bones of a multichannel cochlear implant patient," *Ann. Otol. Rhinol. Laryngol.* **100**, 914–921.